Journey through the world of dynamical systems on networks

M. Cartier van Dissel[1], P. Gora[2], M. Iskrzyński[3], M. Kramar Fijavž[4], D. Manea[5], A. Mauroy[6], I. Nakić[7], S. Nicaise[8], M. Paradowski[9], G. Rotundo[10], A. Puchalska[2], and E. Sikolya[11]

[1] *Complexity Science Hub, Vienna, Austria*
[2] *Institute of Applied Mathematics and Mechanics, University of Warsaw, Warsaw, Poland*
[3] *Systems Research Institute, Polish Academy of Sciences, Warsaw, Poland*
[4] *Faculty of Civil and Geodetic Engineering, University of Ljubljana / Institute of Mathematics, Physics, and Mechanics, Ljubljana, Slovenia*
[5] *Institute of Mathematics, Romanian Academy of Sciences, Bucharest, Romania*
[6] *Department of Mathematics / Namur Center for Complex Systems (naXys), University of Namur, Namur, Belgium*
[7] *Department of Mathematics, University of Zagreb, Zagreb, Croatia*
[8] *University Polytechnique Hauts-de-France, Valenciennes, France*
[9] *Institute of Applied Linguistics, University of Warsaw, Warsaw Poland*
[10] *Department of Statistical Sciences, Sapienza University of Rome, Rome, Italy*
[11] *Department of Applied Analysis and Computational Mathematics, Eötvös Loránd University, Budapest, Hungary*

April 12, 2024

Abstract

We present a subjective selection of methods for complex systems analysis; ranging from statistical tools, through numerical methods based on AI, to both linear and non-linear ODEs and PDEs. All the notions are presented in the context of applied problems to visualise the strengths and drawbacks in the approach. The major aim of capturing such a broad overview is to understand the interrelations between network theories that seem to be distant from the mathematical perspective.

1 Introduction

In the modelling of real life phenomena, the choice of appropriate mathematical tools is the first challenge that one needs to face and is known for its complexity. Striving to accuracy, one heads to incorporate possibly much crucial information about the described process; and, what is

equally important, to eliminate information that influences major aspects of the process in the minor way.

Especially in the fields where social and biological aspects play a role; individual variability, abundance of interconnected sub-components of a phenomenon and uncertainty on their actual interactions, make mathematisation of this branch of science essentially more difficult than for instance in physics. As a consequence, the choice of methods becomes arbitrary and in many cases depends more on the field of expertise of the modeller than on objective reasons. The question on the interplay between different techniques arises naturally and lies in the core of mathematical modelling.

In response to this issue, we propose to examine a bunch of open problems in a wide range of topics such as language studies, finances, ecology, economy, epidemiology or traffic flow. All these questions are bonded by the need to characterise complex dynamics dealing with uncertainty at different description levels. Consequently, a wide range of mathematical methods is applied ranging from statistical analysis, through numerical methods based on AI, to both linear and non-linear ODEs and PDEs. All of them however developed their own mathematical language to incorporate the notion of a network that allows to cluster entities that join certain dynamical properties from one hand, and to state interdependence from another.

The authors do not claim to present either optimal methodology for dealing with presented open problems, or to give the comprehensive summary of toolbox for dynamical systems on network problems. In fact, quite the contrary. Each section is a subjective choice of methods that proved to be useful in dealing with very specific applied problems (presented in Section 2). They are divided based on the type of network that lies in the core of the model and can be assigned to one of four categories (defined formally in Section 3), namely: (combinatorial) digraphs (in Section 4), graphs with dynamics in vertices (in Section 5), metric graphs (in Section 6) and embedded metric graphs (in Section 7).

The picture that emerges from the above description is a wide range of models that offer different ways in the space and time discretisation and vary in connections between modeled subsystems. Even so, one can encounter clear mathematical bridges that fasten some parts of theories with others. It authorises the impression that there are significant similarities in network models that deserve further examination. Our thoughts on these relations being a summary of several discussions engaged among the broad representation of specialists in dynamical systems on networks gathered in the COST Action *Mathematical models of interacting dynamics on networks* can be found in Section 8.

Up to our best knowledge, this is the first paper that encompasses such a broad perspective on the world of dynamical systems on networks. We invite the reader for the journey where we avoid highways of general theories and choose country roads to look in detail into some very specific aspects of arbitrarily chosen topics. We hope that in this round trip many network specialists find the hometown of their expertise. It may be a good starting point for the trip. Depending on the interest of the reader, for some topics window sightseeing might be enough, but in any time one decides for a stopover there are references that direct from this

small snippet to more detailed mathematical study of a topic.

Finally, we hope that making the whole tour brings us closer to the understanding of what are the major factors that should be taken into account when choosing different mathematical apparatus. The wider perspective should highlight gains and loses in the choice of different mathematical settings. Finally, including such different methods in one study indicates that our world of networked dynamical systems is indeed a global village and we can draw inspirations and exchange the concepts one from another. Buon viaggio!

2 Problem descriptions

2.1 Ecology inspiring economy

One of the natural examples of networks in life sciences are food webs. They describe the physical foundation of an ecosystem as mass flows between functional groups of species and their exchange with the environment. They can be regarded as akin to economic networks as both consist of vertices processing and exchanging matter with each other [30, 44]. This enables us to compare properties of these two types of networks and draw inspiration from nature for man-made systems. For example, comparing cycling in these systems is motivated by the goal of a circular economy, that aims to make production processes more sustainable [28, 67]. Such attempts at mimicking food webs were postulated in the context of thermodynamic power cycles [43], industrial parks [42], recycling networks [64, 41], and the whole economy in view of the limits to growth [35]. What can we learn from natural network processes?

2.2 The riddle of language acquisition

Despite recent advances in neural machine translation and large language models, foreign language learning is still a valid goal for large numbers of students. In today's increasingly globalizing world, more and more are deciding to spend at least part of their academic journey at a foreign university. Alongside being attracted by fresh course offerings, the opportunity to travel, experience a new culture and gain new friends, as well as scoring points for their future résumés, one of the chief motivations behind study abroad is advancing one's skills in the language of the target country. However, during their stay abroad not all sojourners make visible linguistic progress, and considerable variation has been evidenced among those that do. It is commonsensical to expect that a crucial role in second language development will be played by students' interaction networks, but how exactly does participants' position/centrality affect their progress across different linguistic competencies [58, 59], what is the impact of the subcommunities/clusters that regularly form in peer cohorts [57], and how do students' language learning trajectories and social behaviors pattern over time [56]?

2.3 Missing data in financial stability modelling

The Bank for International Settlements (BIS) and the related database supports central banks in their pursuit of monetary and financial stability. The related database is owned by 60 central banks and maintained by 48 reporting countries. In 2017 it represented 94% of all the cross-border claims of banks and covered about 95% of the world's Gross Domestic Product. The database [17] is incomplete, since only some estimates can be got from the not−reporting countries. The question is: whether the available dataset is used for estimating the effects of financial contagions, i.e. a cascade failure, is the result reliable? Or, wording it differently, are the missing links playing a relevant role in the contagions dynamic? [15].

2.4 Subscribing the pension plan

Pension funds (PF) need to propose investments based on stock markets for the sustainability of the future pensions. Should a potential subscriber of a specific PF have clear preferences on the reliability of the PF when examining such investments? Are the actual investments an overall good choice for the stability of the PF system? The present work contributes to show how complex network analysis helps to understand the risk involving the whole set of Italian pension funds. In our analysis each pension fund is a network, and its set of investment is reported through a list of declared benchmarks. A link joins two nodes of the network anytime they declare a common benchmark. The detection of communities through the Louvain algorithm and the k-shells show quite a remarkable overlap among the investment of pension funds. These findings show that eventual fluctuations of even a few benchmarks may cause serious consequences in the financial wealth of PF investments, so the system is very fragile [16]. Moreover, the information on the investments of PF based on the stock markets provide very limited hint for the selection of the best PF to subscribe.

2.5 Network identification with missing measurements

Network identification roughly consists in revealing the structure of a graph from data that are generated by agents located at the vertices of the graph and connected to other agents according to the network topology. This problem arises in many contexts, such as neuroscience (e.g. capturing the connections between cerebral regions from brain imaging data), genetics (e.g. inferring gene regulatory networks from gene expression data), social sciences (e.g. measuring influences between individuals on social medias), and finance (e.g. detecting interconnectedness between financial institutions), to list a few. Those situations usually involve large-scale networks, so that measuring all the vertices is out of reach. Moreover, since measurements can possibly be costly or time-consuming, there is a need for methods that only require *local* measurements at a few vertices, but are still capable of revealing *global* topological properties in large networks. Specific problems include, for instance, inferring the average

number of connections between the agents from sparse measurements, detecting a change in the network topology from a remote measurement, and assessing the mutual influence between agents (i.e. community detection).

2.6 Network synchronisation

When a large number of agents are coupled through a complex network of interactions, these interactions lead to cooperative phenomena and emergent properties of the overall dynamical system. An agent can be a model of, for example a ground/underwater vehicle, an aircraft, a satellite, or a smart sensor with microprocessors, while interactions can typically be modelled as an information exchange. An important problem in the study of dynamical systems over networks concerns the emergence of coherent behaviour in which the elements of the system follow some dynamical pattern, i.e. are synchronised. The problems of this type include formation control, flocking, distributed estimation, consensus, and appear in different disciplines, including biology, physics, robotics, and control theory and problems, see e.g. [6]. In the presence of external disturbances of the system, one may want to measure or reduce the impact of disturbances on the synchronisation, and the corresponding problem is called almost synchronisation. Typically disturbances are modelled as stochastic processes, and one uses H_2 or H_∞ norms from systems theory as performance measures of the system. Specific applications include satellite formation flying, distributed computing, robotics, surveillance and reconnaissance systems, electric power systems, cooperative attack of multiple missiles, intelligent transportation systems, and neural networks.

2.7 Tracing virus' variants in fragmented environment

In 2019, due to the outbreak of SARS-CoV-2 pandemics, the problem of monitoring the spread of infectious disease changed into a global challenge. In the first years of pandemics the major question was to estimate properly the real number of colonised and infected patients in order, first, to estimate the basic reproduction number, known as $\mathcal{R}_0$ parameter, and in the consequence, to navigate wisely in policy responses. Since December 2020, when the first COVID-19 vaccine has been released, more and more attention has been focused on the problem of tracing the new variants, in particular those whose response to the vaccine is weaker. Modelling the prevalence of patients colonised by the particular variant of a SARS-CoV-2 virus in the local environment allows for either the production of more tailor-made vaccines, similarly to flu vaccines, or at least for the wider availability of this among different vaccine that should be more efficient for particular groups of patients.

2.8 Optimizing road traffic

Urban road transport poses significant challenges to civilization and economic activity, impacting quality of life and productivity. Addressing

these issues requires interdisciplinary approaches and sustainable urban planning strategies to alleviate traffic-related negative effects. One such approach involves optimizing traffic signal settings for given traffic conditions, but this problem has been proven to be NP-hard even for relatively simple traffic models [13]. Also, even evaluating the quality of different traffic signal settings can be time-consuming, especially on a large scale. Therefore, there is a need to develop new traffic modeling and optimization methods.

3 Preliminary network description

3.1 Combinatorial digraphs

The basic object of our consideration is a *digraph* (known also as *directed graph*) $G = (V, E, \Phi^{\pm}, W)$ with sets of *vertices* $V = \{v_i\}_{i\in I}$, $I = \{1, \ldots, n\}$, and *edges* $E = \{e_j\}_{j\in J} \subset V \times V$, $J = \{1, \ldots, m\}$. The graph structure is encoded by *in- and out-incidence matrices* $\Phi^{\pm} = (\phi^{\pm}_{i,j})_{i\in I, j\in J}$ defined as

$$\phi^{+}_{ij} = \begin{cases} 1 & \text{if} \quad \overset{e_j}{\to} v_i, \\ 0 & \text{otherwise,} \end{cases} \qquad \phi^{-}_{ij} = \begin{cases} 1 & \text{if} \quad v_i \overset{e_j}{\to}, \\ 0 & \text{otherwise,} \end{cases} \tag{1}$$

and a *weight matrix* $W = \mathrm{diag}(w_j)_{j\in J}$, $w_j > 0$, $j \in J$.

If all weights are equal, we call G an *unweighted digraph*. By a *(undirected) graph* we understand a digraph having a property that for any $(v_i, v_j) \in E$, $(v_j, v_i) \in E$. We also denote by $E^{\pm}_{v_i}$ sets

$$E^{+}_{v_i} = \{e_j \in E : \overset{e_j}{\to} v_i\}, \qquad E^{-}_{v_i} = \{e_j \in E : \ v_i \overset{e_j}{\to}\},$$

and their weights' counterparts $W^{\pm}_{v_i}$

$$W^{\pm}_{v_i} = \{w_j : \ e_j \in E^{\pm}_{v_i}\}, \qquad W_{v_i} = W^{+}_{v_i} + W^{-}_{v_i}. \tag{2}$$

If $e_k = (v_i, v_j) \in E$ then v_i is a *tail* and v_j is a *head* of an edge. We say that a vertex $v_i \in V$ is a *source* (resp. a *sink*) if $\sum_{j\in J} \Phi^{+}_{ij} = 0$ (resp. $\sum_{j\in J} \Phi^{-}_{ij} = 0$). Furthermore, e_j is a *loop* if there exists $v_i \in V$ being both its head and tail. By the *multiple edge* in the digraph we understand at least two edges all having a head in $v_i \in V$ and a tail in $v_j \in V$. By the l-length *path* in the graph we understand a sequence of edges $e_1, e_2, \ldots, e_l$, $e_i \in E$, $i = 1, \ldots, l$; such that for each $i = 1, \ldots, l$, there exists $k_i \in I$ such that $\phi^{+}_{k_i i} = \phi^{-}_{k_i i+1}$. We say that a digraph is connected if for any two vertices $v_i, v_k \in V$ there exists a path such that its first edge has a tail in v_i and the last edge has a head in v_k.

In this paper we restrict our consideration to connected digraphs having a finite number of vertices and edges, and no multiple edges (loops are allowed).

When considering the dynamics in the vertices of digraphs it is convenient to define operators between vertices. By *weighted in- and out-adjacency matrices*, $\mathcal{A}^{\pm}_{w} = (a^{w\pm}_{ij})_{i,j\in I}$, $(\mathcal{A}^{+}_{w})^T = \mathcal{A}^{-}_{w}$, we understand

$$a^{w+}_{ij} = \begin{cases} w_k & \text{if} \quad \exists_{e_k\in E}\ v_j \overset{e_k}{\to} v_i \\ 0 & \text{otherwise.} \end{cases}$$

If we replace $a_{ij}^{w\pm} \neq 0$ with $a_{ij}^{\pm} = 1$, we say that $\mathcal{A}^{\pm} = (a_{ij}^{\pm})_{i,j\in I}$ is an *(unweighted) in- and out- adjacency matrix.*

To give the number of edges entering or going out from the vertex and their cumulative weight we define respectively *(unweighted) in- and out-degree matrices* $\mathcal{D}^{\pm} = \mathrm{diag}(\deg^{\pm}(v_i))_{i\in I}$ and *weighted in- and out-degree matrices* $\mathcal{D}_w^{\pm} = \mathrm{diag}(\deg_w^{\pm}(v_i))_{i\in I}$

$$\deg^{\pm}(v_i) = \sum_{j\in J} \phi_{ij}^{\pm}, \qquad \deg_w^{\pm}(v_i) = \sum_{j\in J} \phi_{ij}^{\pm} w_j. \tag{3}$$

The *undirected unweighted adjacency matrix* is defined as

$$\mathcal{A} = \mathcal{A}^{+} + \mathcal{A}^{-}, \tag{4}$$

and the *unweighted degree matrix* as

$$\mathcal{D} = \mathcal{D}^{+} + \mathcal{D}^{-}, \tag{5}$$

while *undirected weighted adjacency matrix* by

$$\mathcal{A}_w = \mathcal{A}_w^{+} + \mathcal{A}_w^{-}. \tag{6}$$

Let us also mention two other basic operators that are used to characterise the dynamics associated with vertices, namely advection and Laplacian matrix. In the case of directed graphs they can be defined at various ways and consequently one can find many names of the same objects. In this paper we mostly follow the notation from [51]. Hence, *weighted in- and out-advection matrices* are $\mathcal{N}_w^{\pm} = (N_{w,ij}^{\pm})_{i,j\in I}$ such that

$$\mathcal{N}_w^{+} = \mathcal{D}_w^{-} - \mathcal{A}_w^{+}, \qquad \mathcal{N}_w^{-} = \mathcal{D}_w^{+} - \mathcal{A}_w^{-}. \tag{7}$$

While, by *weighted in- and out-degree Laplacian matrix* $\mathcal{L}_w^{\pm} = (L_{w,ij}^{\pm})_{i,j\in I}$ (known also as *incoming and outgoing Kirchhoff matrix* and denoted by $\mathcal{K}_w^{\pm} = (K_{w,ij}^{\pm})_{i,j\in I}$) we understand

$$\mathcal{L}_w^{+} = \mathcal{K}_w^{+} = \mathcal{D}_w^{+} - \mathcal{A}_w^{+}, \qquad \mathcal{L}_w^{-} = \mathcal{K}_w^{-} = \mathcal{D}_w^{-} - \mathcal{A}_w^{-}. \tag{8}$$

Finally, by $\mathcal{L}_w^{B} = (L_{w,ij}^{B})_{i,j\in I}$ we denote *weighted Laplacian-Beltrami matrix*, namely

$$\mathcal{L}_w^{B} = \mathcal{L}_w^{+} + \mathcal{L}_w^{-}. \tag{9}$$

To obtain unweighted counterparts of advection $\mathcal{N}^{\pm} = (N_{ij}^{\pm})_{i,j\in I}$, Laplacian $\mathcal{L}^{\pm} = (L_{ij}^{\pm})_{i,j\in I}$ (known as Kirchhoff $\mathcal{K}^{\pm} = (K_{ij}^{\pm})_{i,j\in I}$) and Laplacian-Beltrami matrices we consider unweighted degrees $\mathcal{D}^{\pm}$ and unweighted adjacency matrices $\mathcal{A}^{\pm}$ in formulas (7), (8); as well as unweighted Laplacians in (9).

Finally, when considering the dynamics defined on digraphs' edges it is convenient to also define operators between edges. A *weighted in-adjacency matrix of a line graph of* G we call a matrix $\mathcal{B}_w^{\pm} = (b_{w,ij}^{\pm})_{i,j\in J}$ such that

$$b_{w,ij}^{+} = \begin{cases} w_j & \text{if } \exists_{v_k\in V} \overset{e_j}{\to} v_k \overset{e_i}{\to} \\ 0 & \text{otherwise.} \end{cases}$$

$$b_{w,ij}^{-} = \begin{cases} w_i & \text{if } \exists_{v_k\in V} \overset{e_j}{\to} v_k \overset{e_i}{\to} \\ 0 & \text{otherwise.} \end{cases}$$

In the case of *unweighted adjacency matrix* $\mathcal{B} = (b_{ij})_{i,j\in J}$ *of a line graph of* G, we consider $b_{ij} = 1$, when $b^{\pm}_{ij} \neq 0$, and $b_{ij} = b^{\pm}_{ij}$ otherwise.

3.2 Metric graphs

The second major group of networks used in the modelling of dynamical systems are metric graphs. This concept is the generalisation of digraph that allows to associate each edge with one dimensional metric space and consequently define differential operators on the network.

Using mathematical formalism, let $\mathcal{G} = (G, d)$ be a *metric graph* where $G = (V, E, \Phi^{\pm}, W)$ is a digraph defined in Section 3.1 and $d : E \to \mathcal{B}(\mathbb{R})$, for $\mathcal{B}(\mathbb{R})$ being the Borel σ-algebra, is a mapping of a form $e_j \mapsto [0, l_j]$, $l_j > 0$ for any $j \in J$. Note that $E = \{e_j\}_{j\in J} \subset V \times V$, is a set of edges of digraph and $J = \{1, \ldots, m\}$.

In the metric graph the direction of an edge $e_j = (v_i, v_k) \in E$, $i, k \in I$, can be associated with the parametrisation of $d(e_j)$ hence by abuse of notation we denote a tail (resp. head) of an edge e_j by $e_j(0) = v_i$ (resp. $e_j(l_j) = v_k$).

In the metric graph models the state space consists of edges that are joined together by vertices in which they start and end. Finally, we head to associate the network with the space it is embedded into. We say that a digraph $G = (V, E, \Phi^{\pm}, W)$ is a *planar digraph* if it can be drawn on the plane in such a way that its edges intersect only at their endpoints. For every such network we can chose its planar representation defining for a chosen $v_0 \in V$ a mapping $P_{v_0} : \{v_0\} \times E \to \mathbb{R}^2 \times [0, 2\pi)^m$ such that

$$P_{v_0} : \ (v_0, e_1, \ldots, e_m) \mapsto (x, y, \alpha_1, \ldots, \alpha_m) \tag{10}$$

associates a vertex v_0 with a point (x, y) as its representation on the plane, while α_j gives an angle of edge e_j with respect to Ox axis. We say that $G_P = (V, E, \Phi^{\pm}, W, P_{v_0})$ is a *planar embedding of a digraph* $G = (V, E, \Phi^{\pm}, W)$, while $\mathcal{G}_P = (G_p, d)$ is a *planar embedding of a metric graph*.

Finally, in the whole article we use the notation

$$I_n \in \mathbb{R}^{n\times n}, \quad \mathbb{1}_n = [1, \ldots, 1]^{\top} \in \mathbb{R}^n, \tag{11}$$

respectively, for identity matrix and vector that consist of all entries equal to one.

4 Combinatorial digraphs

In this section statistical tools are applied to reveal the information encoded in the network structures. The authors consider the graphs measures which are the parameters that characterise certain properties of a digraph: node degree, closeness, betweenness, pagerank, reciprocity or Finn cycling index to mention a few. Another approach is to extend the deterministic notion of a digraph into the Erdös–Renyi random structure or Barabasi–Albert scale free networks.

4.1 Networked ecosystems and economies

Studying the flow and cycling of matter in networks is crucial for understanding the fundamental physical structure of both ecosystems and economies. Food webs describe how biomass moves between groups of species in ecosystems, arising mostly from feeding relationships. Similarly, input-output tables capture the flow of goods and services between industries and consumers in an economy. In [33], 169 weighted food webs and 155 economic networks are compared based on the fraction of total system throughflow that is cycled, known as the Finn Cycling Index (FCI).

In order to learn more about quantification of mass' cycles let us consider both food webs and economic networks as weighted digraphs $G = (V, E, \phi^{\pm}, W)$, see Section 3.1, with weights W denoting the flow of matter along edges. In this study the vertices are in addition characterised by external export from each vertex $o = (o_i)_{i\in I}$, where $o_i \geq 0$.

The amount of matter leaving a node $v_i \in V$, denoted by $h = (h_i)_{i\in I}$, is assumed to be positive and is given by

$$h_i = \sum_{j=1}^{n} a_{ji}^{w+} + o_i > 0.$$

A transition matrix $C = (c_{ij})_{i,j\in I}$ describes a probability that a unit of mass moves between adjacent nodes, namely

$$c_{ij} = \frac{a_{ij}^{w+}}{h_j} \quad \text{for any } i, j \in I.$$

Finally, in order to include indirect flows between nodes one defines overall transition probability $U = (u_{ij})_{i,j\in I}$ as the power series

$$U = \sum_{q=0}^{\infty} C^q = (I_n - C)^{-1}.$$

Matrix U is well-defined since C is sub-stochastic.

The Finn Cycling Index (FCI), see [26], of a vertex is the probability that flow passing through a node returns (via direct or indirect flow) to it at some time point, formally:

$$\mathrm{FCI}_i = \frac{u_{ii} - 1}{u_{ii}}, \quad \text{for any } i \in I.$$

Note that $u_{ii} \geq 1$ from the definition, and therefore FCI is a measure that ranges from 0 to 1. A value of FCI = 0 indicates that there are no directed cycles in the system, meaning that no flow originating from any node returns to the same node through any path. Conversely, a value of FCI $= \mathbb{1}_n$, see (11), represents a system in which all flows eventually return to their starting node.

The most basic form of cycling occurs when two nodes exchange mass reciprocally. The network *reciprocity* r measures the fraction of such overlapping bilateral flows among all flows:

$$r = \frac{\sum_{i,j\in I} \min[u_{ij}, u_{ji}]}{\sum_{k,l\in I} u_{kl}} \in [0, 1].$$

If all flows are perfectly reciprocated, then $r = 1$. Whereas if there are no nodes connected by flows in both directions we have $r = 0$.

The turns out that the FCI of food webs has a geometric mean of 5%, with much of the cycling attributed to reciprocal flows and the recycling of dead organic matter by detritivores. In contrast, the global economy in 2011 had an FCI of 3.7%. Furthermore, [33] highlights that unweighted network measures used in the past, such as the largest eigenvalue of the adjacency matrix, do not correlate with the actual cycling in weighted networks.

Interestingly, both food webs and economic networks exhibited a strong correlation between FCI and reciprocity, defined as the fraction of flow that is immediately returned between two nodes. This suggests that promoting reciprocity and local collaboration between network components could be a simple strategy to enhance cycling without requiring global knowledge of the system structure. The study emphasizes the importance of relying on weighted network indicators to make sound inferences about real-world systems.

A related work [62] developed an open-source Python package called foodwebviz for visualizing weighted food webs. The package offers five complementary methods: 1) a heat map of flows or diet proportions, 2) an interactive graph for tracing matter flow, 3) an intuitive animation of particles moving between nodes, 4) a summary bar plot of trophic level exchanges, and 5) a heat map of trophic level flows. These tools facilitate accompanying food web publications with clear, aesthetically appealing visualizations that can engage the broader public and be incorporated into education.

Together, these studies contribute to our understanding of mass cycling in complex networks and provide practical tools for their analysis and communication. They highlight the insights gained from weighted network approaches and the potential for local strategies to enhance sustainability in both ecosystems and economies.

4.2 Peer interactions and second language acquisition during study abroad

In today's increasingly globalizing world, more and more students are deciding to spend at least part of their academic journey at a foreign university. In this section of a paper we study conductive factors to second language (L2) development as well as possible barriers. We are also interested in the time evolution of students' language learning trajectories and social behaviors patterns.

Social network analysis (SNA) offers a successful line of inquiry permitting answers to these questions [18, 31, 36, 49, 50, 58, 59, 57]. Particularly fruitful have been computational analyses that go beyond investigations of egocentric networks and instead attempt to reconstruct possibly complete learner graphs. In this vein, an analysis of a cohort of Erasmus+ students at a university in Germany demonstrates the potential of cluster detection algorithms, revealing the deleterious influence on language acquisition of the formation of subcommunities composed of co-nationals and other

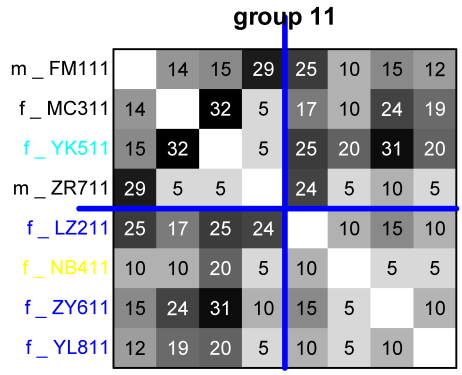

Figure 1: Class of students enrolled in an intensive course of the Polish language and culture showing clear partitioning along shared languages, German and Russian.

speakers of the same native language, and the negative impact of *closeness centrality*, suggesting the advantage of maintaining fewer high-quality interactions over several necessarily more superficial ones [57].

SNA also helps unearth heterophily in L2 German proficiency levels among favorite contacts, revealing the understandably negligent impact of this criterion in choosing friends, and the importance of the proportion of using the target language vs merely being exposed to it passively. Additional research in two iterations of a large-scale course of the Polish language and culture in Warsaw revealed how the centrality metrics best predicting measurable progress are *closeness* and degree with outdegree, see (3), and *betweenness* also explaining subjectively perceived headway in vocabulary and pronunciation [58, 59].

The study also showed background-language-based homophily among students frequently interacting with one another, with clusters in the stochastic blockmodels often aligning with learners' shared languages (Figure 1).

The static data have already given us some knowledge, but what if we are interested in whether observable changes can be noticed in the patterns of students' social interaction over time? Questions concerning the changing dynamics of second language development and peer communication can be answered employing longitudinal network analyses with several time points/snapshots; a new SNA paradigm in quantitative L2 research.

One recent project followed a full group of 41 U.S. students enrolled in an intensive 3-month semester-long Arabic program in Amman, measuring their social interaction and progress after every four weeks. The findings revealed relative stability in terms of students' positions in the network, with a stable tendency to form cliques with peers of the same gender (Figure 2), and the gender homophily strengthening with time [56]. The results also showed that three out of five predictors of objec-

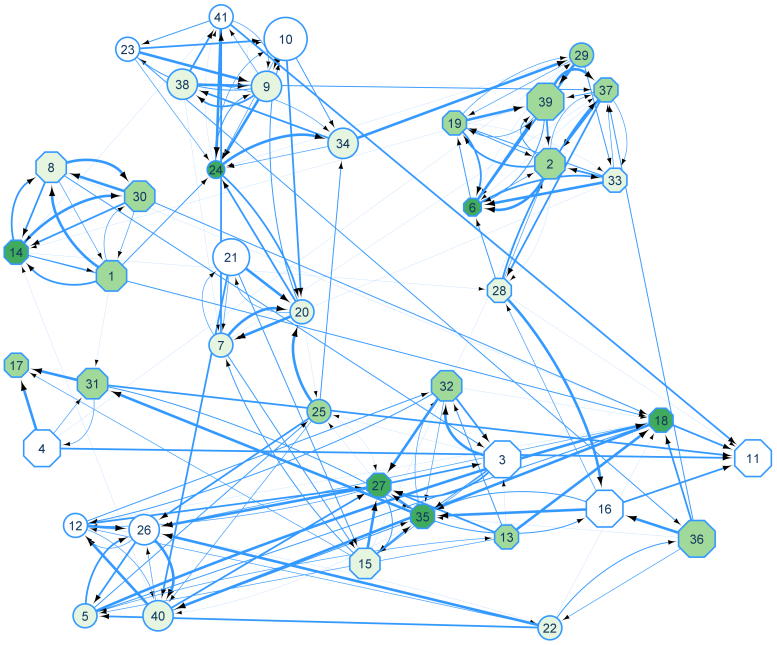

Figure 2: Students' interactions during the middle month of their sojourn abroad.

tive progress were connected with social interaction (*indegree*, *pagerank*, and perception of group integration), that presojourn proficiency in Arabic negatively influenced initiating interactions in this language, and that female students were spending considerably more time with their alma mater classmates.

Network science has also led to epistemological contributions in other fields of linguistics [34], shedding light on phenomena such as the social diffusion of innovation, or the relationships between constructs in educational psychology. For instance, investigating the spread of neological tags online, [61] showed the benefits of gaining authorized backend access to an entire microblogging site, thus permitting insight into the degree of the "saturation" of the system rather than merely raw numbers of occurrences of the expression of interest, revealing how resistance against the adoption of novelty concentrates around relatively low values, that the vast majority of the users are moderately innovative, and that the spread of the most popular tags may be taking place during most users' offline time. Language education research has also benefited from psychologi-

cal network analysis [22], a variable-centered relation-intensive approach helpful in visualizing relationships between constructs and estimating the relative importance of factors in complex networks of associations. This type of network analysis has so far received relatively little attention from linguists [27], but has already been used e.g. to provide insight into the relationship between grit and its non-trivial predictors in online language learning [60].

4.3 Network identification from BIS database

The process of decision−making is often based on the information available through databases that unfortunately in many cases are proven to be incomplete. The present analysis, following the results in [15], aims at understanding how bad is the missing information in the Bank for International Settlements (BIS) database arising due to the existence of non-reporting countries.

In the research gathered data are used to build up a digraph G, where the countries are the nodes, and the weights of the directed links report positive cross-border exposure. A contagion dynamics is set up considering two possible states of a node v_j connected to a node v_i: either Credit (the node v_j has a positive credit to the node v_i) or Debt (the node v_j has a debt to the node v_i) and two possible events on the node v_i: either Loss (the node v_i loses value) or Gain (the node v_i gains value). At first, simulations are performed on the original BIS network, and on simulated *random networks* (Erdos-Renyi) and *scale free* (Barabasi-Albert model). As a second step, the total number of links in each network is increased in two different ways: either at random, or adding more links among the nodes which are less connected ('organizer periphery').

The analysis performed clearly shows that incomplete data lead to misleading information about robustness of the network. The increase of links supposed to be missing increases the magnitude of the contagion; moreover, the effect is at its worst in the case of organized peripheral. The main conclusion is that the usage of the database as it is may lead to potentially biased actions which could not achieve the goal of stabilizing the system.

4.4 Would you subscribe my pension plan?

Pension funds (PF) account for quite a remarkable amount of the Gross Domestic Product, which in the OECD area averages at 50.7%. The way in which pension funds are able to pay the pensions is through investments. We focus the analysis on the similarity among the investments according to the selection of the investments on risky assets from the financial markets, and are referred through the declared benchmark. Although the economic relevance is clear, the literature on the PF is quite limited. Our aim is understanding the similarities among the PF through tools and measures proper of the complex networks approach.

The starting point is building the undirected graph G in which nodes $v_i \in V$, $i \in I$, are the pension funds while edges' weights w_j, $j \in J$, mea-

sure the overlap among pension funds due to the overlap on the benchmarks, with

$$W_V = \sum_{j \in J} w_j$$

being the sum of all weights in this network. For that, consider the database reporting the Italian pension funds and the declared benchmarks. Data has been provided by MEFOP (Italian Ministry) and refers to the year 2017. The set includes 61 active sub-funds (belonging to 49 funds) with their 72 self-declared benchmarks. Data has been crosschecked through the Bloomberg database. Our analysis focuses on *open pension fund* (the one that anybody can subscribe to). Let $H = (h_{il})_{i \in I, l \in L}$ be a matrix reporting the pension funds on the rows and the benchmarks on the columns. $h_{ij} \geq 0$ is the percentage of the investment of the fund v_i in the pension fund for a benchmark j. Let $\mathcal{A}_w = (a_{ij}^{w\pm})_{i,j \in I} = H \cdot H^T$ be a weighted undirected adjacency matrix, see (6), of a digraph G. In complex networks literature this matrix is known as *one–mode projection*. Note that the object is well-defined since both rows and columns of $\mathcal{A}_w$ are the pension funds. We are going to explore similarities through the application of two clustering methods *the Louvain method* and the *k-shells*.

The Louvain method for community detection follows a bottom-up approach in which the nodes forming subnetworks as close as possible to complete subnetworks are gathered together. More formally, let us consider a division of a graph G into subnetworks $\{G_l : \ l \in L\}$ and define a Dirac function $\delta : V \times V \to \{0, 1\}$, such that $\delta(v_i, v_j) = 1$ when v_i, v_j are in the same subnetwork. One optimizes the modularity related to the division

$$Q\left(\{G_l : \ l \in L\}\right) = \frac{1}{2W_V} \sum_{i,j \in I} \left[a_{ij}^w - \frac{W_{v_i} W_{v_j}}{2W_V} \right] \delta(v_i, v_j),$$

where W_{v_i}, W_{v_j} are the sums of the weights of the edges attached to nodes v_i and v_j respectively, see (2) for definition.

The k-shell of order k is defined as the set of nodes which have degree at least n after all the nodes with degree at maximum $k-1$ have been removed. The procedure for the identification of the k shell is iterative. The higher is k, the higher is the connection among the nodes in the same shell.

The Italian open pension funds resulted to be quite strongly connected. The Louvain method distributes them across all the communities; a subgroup is also in the same community of the *contractual* pension funds, which are intended to specific categories of workers, that can be set up on the basis of collective agreements. The k-shell method confirms the results of the Louvain method to a large extent.

5 ODEs on combinatorial graphs

In this section, we consider dynamical systems over networks (DSN), also called networked dynamical systems. Let us consider a (large) number n of

agents in interaction. Each agent indexed by i is described by its internal state x_i which evolves in time both because of an internal dynamics and because of the coupling with the other units. A quite general form to describe the evolution of the system is given by the set of equations

$$\dot{x}_i = F_i(x), \tag{12}$$

where $x = (x_1, \ldots, x_n)$. The set of agents and their evolution equations (12) can be seen as a digraph $G = (V, E, \phi^{\pm}, W)$, see Subsection 3.1, and two vertices v_i and v_j are linked by a directed edge from v_j to v_i if the evolution equation of the agent i depends on the state x_j of the agent j.

We will focus on DSNs that consist of identical agents (or units) interacting through a diffusive coupling:

$$\dot{x}_i \;=\; F(x_i) + G(x_i) \sum_{k\,=\,1}^{n} a^{+}_{ik} H(Q(x_i) - Q(x_k)) \qquad x_i \in \mathbb{R}^p,\, i \in I, \tag{13}$$

with the functions $F : \mathbb{R}^p \to \mathbb{R}^p$ such that $F(0) = 0$, $G : \mathbb{R}^p \to \mathbb{R}^{p\times r}$, $H : \mathbb{R}^q \to \mathbb{R}^r$, and $Q : \mathbb{R}^p \to \mathbb{R}^q$ such that $Q(0) = 0$. Coefficients a^{+}_{ik}, $i, k \in I$ are the entries of a matrix $\mathcal{A}^{+}$, namely unweighted in-degree adjacency matrix of G defined Section 3.1.

5.1 Network synchronisation

Here we will deal with output synchronisation problem, which can be described as follows. Let the states of DSN be described by eq. (13) with the underlying network structure described by the graph G and with the corresponding agent outputs given by

$$y_i = Q(x_i). \tag{14}$$

The goal of the output synchronisation [45] is to reach asymptotic agreement between all agents, i.e.

$$\lim_{t\to\infty} (y_i(t) - y_j(t)) = 0, \quad \text{for all } i, j \in I. \tag{15}$$

One can look at this notion as a natural replacement of stability for dynamical systems on networks. Indeed, take $F = 0$, $G = H = Q = 1$ in eq. (13). Then the DSN corresponds to a so-called network of single-integrators or a network without internal dynamics

$$\dot{x}_i = 0,\; i \in I,$$

coupled by the linear feedback with outputs being the states of the agents. This system is invariant to translations, i.e. if we translate the initial conditions $x_i(0)$ of all agents by the same amount, the differences between the states will not change. One can easily check this by noting that the vector $\mathbb{1}$, see (11), is the (right) eigenvector of $\mathcal{L}^{+}$. The same holds for DSNs of double-integrators and other important systems. This implies that such systems are always unstable and asymptotic stability does not

hold. As an example, let us consider a general linear DSN with second order dynamics in vertices. Let

$$\ddot{x}_i = -A\dot{x}_i + Bu_i, \quad y_i = \begin{bmatrix} x_i \\ \dot{x}_i \end{bmatrix}$$

where (A, B) is a stabilizable pair, and u_i is the coupling given by

$$u_i = -\begin{bmatrix} C_1 & C_2 \end{bmatrix} \sum_{k=1}^{n} a_{ik}^{+} \left(\begin{bmatrix} x_k \\ \dot{x}_k \end{bmatrix} - \begin{bmatrix} x_i \\ \dot{x}_i \end{bmatrix} \right).$$

Then the system matrix is given by

$$\mathcal{C} = \ I_{2n} \otimes \begin{bmatrix} 0 & I_n \\ 0 & -A \end{bmatrix} - \mathcal{L}^{+} \otimes \begin{bmatrix} 0 & 0 \\ -C_1 & -C_2 \end{bmatrix}.$$

It is easy to check that the kernel of $\mathcal{C}$ contains the vectors of the form $\mathbb{1} \otimes [v\ 0]^{\top}$ and the system is again invariant to translations.

In the presence of exogenous disturbances w_i of the agents, one would like to make the norm of the mapping $\bar{y} \mapsto y_i - y_j$ smaller than some given tolerance γ, where $\bar{y} = [\bar{y}_1 \ \dots \ \bar{y}_n]$.

Typical choices for norms are H_2 and H_∞, as both norms measure the impact of exogenous disturbances given in the form of a stationary stochastic process. To be more precise, the H_2 norm can be interpreted as the output variance for disturbances described by a white noise, while the H_∞ norm measures the worst-case effect a disturbance can make on the system, see [19]. In this setting we talk about H_2/H_∞ *almost output synchronisation*.

If the underlying graph is undirected and connected, then one can transform the system, without loss of information, to a system with stable system matrix. Indeed, then $\mathcal{L}^{+} = \frac{1}{2}\mathcal{L}$ is symmetric and $\mathbb{1}$ spans the kernel of $\mathcal{L}$. Let the matrix Y be such that its columns span the subspace $\{\mathbb{1}\}^{\perp}$ and such that $Y^{\top}Y = I$. If we define $Z = Y \otimes I$ then the substitution $x = Zx'$ defines a reduced system with a stable system matrix. From the solution of the reduced system one can recover the state of the original system up to translation invariance.

In the case of a directed graph G, the situation is more complicated. In general, the vector $\mathbb{1}$ is only going to be a *left* eigenvector corresponding to the eigenvalue zero. For example, the in-degree Laplacian of the following simple digraph

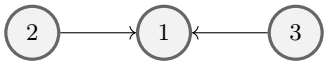

has (algebraic and geometric) multiplicity 2. Hence, a reduction similar to the one described for undirected graphs is not possible as we would lose too much information. Moreover, the corresponding DSN will not have the property of output synchronisation. This can be easily seen by investigating a network without internal dynamics. The solution of the corresponding ODE is given by $x(t) = \mathrm{e}^{-\mathcal{L}^{+}t}$ where

$$\mathcal{L}^{+} = \begin{bmatrix} 2 & 0 & 0 \\ -1 & 0 & 0 \\ -1 & 0 & 0 \end{bmatrix},$$

and one obtains $|x_2(t) - x_1(t)| \to \infty$ as $t \to \infty$ if $x_2(0) \neq 0$. The issue with this system is that both "leader" vertices 2 and 3 are influencing the "follower" vertex 1. It is clear that such couplings will always lead to pathological systems. So the relevant DSNs are those where the graph G is a *directed forest*, i.e. a union of directed trees (subgraphs of the graph G in which there exists a unique path from the root vertex to each node in this subgraph). Obviously, this means that it is sufficient to analyse graphs which contain a spanning directed tree and indeed this is a standard assumption in the literature.

To quantitatively analyse the output synchronisation property, one can ask the following question: if one is able to disturb/bolster merely one vertex in order to maximally disturb/bolster the entire system, which vertex to choose? This question is obviously related to the almost output synchronisation property, and in this way one can find an ordering of vertices according to their sensitivity to the external disturbances. In the case of undirected graphs with double-integrators in the vertices and H_∞ norm, this can be efficiently calculated as shown in [52]. Similar analysis can be made for general systems of identical linear agents.

5.2 Spectral network identification

Network identification with few measurements (see Section 2.5) can be tackled through spectral methods. On the one hand, it is well-known from spectral graph theory that the eigenvalues of Laplacian matrices $\mathcal{L}^{\pm}$, see (8), (hereafter called *Laplacian eigenvalues*) provide meaningful information on the topological structure of the graph, such as the mean vertex degree [14]. Moreover, changes in the spectrum of the Laplacian matrix reveal changes in the graph structure, and communities can also be inferred from the Laplacian eigenvectors. On the other hand, the spectrum of the so-called Koopman generator[1]

$$A_G : \mathcal{D}(A_G) \to \mathcal{F}, \quad A_G f = \bar{F}_G \cdot \nabla f,$$

where $\mathcal{F}$ is a Banach space and $\bar{F}_G$ is a vector field describing an ODE over a graph G, can be estimated from data generated by the dynamics (see e.g. the Dynamic Mode Decomposition (DMD) method [65]) and measured at a few vertices (possibly one). Therefore, providing that the Laplacian spectrum can be retrieved from the Koopman operator spectrum, the *global structure* of the graph can be inferred through *local measurements* of the dynamics.

In other words, network identification with a few measurements is equivalent to the *spectral network identification* problem, defined as follows. Considering the set of all graphs G with a fixed number of vertices, we aim at studying the existence of a correspondence between the set $\mathcal{S}_A$ of point spectra, $Sp_p(A_G)$ of the Koopman generators A_G, and the

[1] In well-chosen spaces (depending on the dynamics), the operator A_G is the infinitesimal generator of the strongly continuous semigroup of Koopman operators $(K^t)_{t\geq 0} : \mathcal{F} \to \mathcal{F}$ defined by the composition $(K^t)f(\cdot) = f \circ \varphi(t, \cdot)$ where $\varphi : \mathbb{R}^+ \times X \to X$ is the flow map generated by the dynamics [11, 37].

set $\mathcal{S}_{\mathcal{L}^+}$ of spectra $Sp(\mathcal{L}^+)$ of the in-degree Laplacian matrix $\mathcal{L}^+$ of the graphs G.

We now focus on the specific DSN (13). The Jacobian matrix $J \in \mathbb{R}^{np\times np}$ of the vector field at the origin is given by

$$J = I_n \otimes B - \mathcal{L}^+ \otimes C$$

where I_n identity matrix, see (11), $B = J_F \in \mathbb{R}^{p\times p}$ is the Jacobian matrix of F, and $C = G(0)J_H(0)J_Q(0)$, with $J_H \in \mathbb{R}^{r\times q}$ and $J_Q \in \mathbb{R}^{q\times p}$ the Jacobian matrices of H and Q, respectively. We assume that J has non-resonant eigenvalues μ_j $(j = 1, \dots, np)$ with $\Re\{\mu_j\} < 0$, so that the origin is an asymptotically stable synchronised equilibrium. In this case, the point spectrum of the Koopman generator A defined in the Hardy space $\mathcal{F} = H^2(\mathbb{D}^{np})$, where $\mathbb{D}^{np} \subset \mathbb{C}^{np}$ is a polydisk of radius small enough, is given by

$$Sp_p(A) = \left\{ \sum_{j=1}^{n} \alpha_j \mu_j,\, \alpha \in \mathbb{N}^n \right\} \supset Sp(J).$$

It follows that there is a one-to-one correspondence between the set of spectra $\mathcal{S}_A$ and the set $\mathcal{S}_J$ of spectra $Sp(J)$, so that the problem boils down to an algebraic characterisation of the correspondence between the sets $\mathcal{S}_J$ and $\mathcal{S}_{\mathcal{L}^+}$. We have the following result based on the spectral moments of the matrix C [29].

Proposition 1. *Consider two in-degree Laplacian operators $\mathcal{L}_1^+$, $\mathcal{L}_2^+$ associated with two digraphs G_1, G_1. If $\mathrm{tr}(C^k) \neq 0$ for all $k \in \{1, \dots, n\}$, then there is a one-to-one mapping between $\mathcal{S}_J$ and $\mathcal{S}_{\mathcal{L}^+}$, that is*

$$Sp(J_1) = Sp(J_2) \Leftrightarrow Sp(\mathcal{L}_1^+) = Sp(\mathcal{L}_2^+)$$

with $J_1 = I_n \otimes B - \mathcal{L}_1^+ \otimes B$ and $J_2 = I_n \otimes B - \mathcal{L}_2^+ \otimes C$.

Moreover, the spectrum of J can be easily expressed in terms of Laplacian eigenvalues.

Lemma 1. *The spectrum of $J = I_n \otimes B - \mathcal{L}^+ \otimes C$ is given by*

$$Sp(J) \;=\; \bigcup_{\lambda \in Sp(L^+)} Sp(B - \lambda C).$$

Proof. Let P be the matrix constructed with (generalised) eigenvectors of $\mathcal{L}^+$, such that $P^{-1}\mathcal{L}^+P$ has a Jordan form. Then the matrix $\tilde{J} = (P\otimes I_n)^{-1}J(P\otimes I_n) = \mathrm{diag}(M_1, \dots, M_r)$ is block-diagonal, with the blocks $M_j = I_{\mathrm{rank}(J_\lambda)} \otimes B + J_\lambda \otimes C$, where J_λ is a Jordan block associated with an eigenvalue $\lambda \in Sp(\mathcal{L}^+)$, and $\mathrm{rank}(J_\lambda)$ is its rank. It is clear that the matrices M_j are block triangular, with diagonal blocks $B + \lambda C$. This implies that $Sp(M_j) = Sp(B + \lambda C)$ and the result follows from the fact that $Sp(J) = Sp(\tilde{J}) = \cup_{j=1}^{r} Sp(M_j)$. □

It follows from Lemma 1 that the Laplacian eigenvalues λ can be obtained from the eigenvalues $\mu \in Sp(J) \subset Sp_p(A)$ by solving the generalised eigenvalue problem

$$(B - \mu I_n)v = \lambda C v.$$

For a given eigenvalue $\mu \in Sp(J)$, there are as many solutions λ as the rank of C, but only one solution is a Laplacian eigenvalue. Specific techniques have to be developed to circumvent this issue (see [29] for more details).

When the matrix C has rank one (e.g. in the case $r = 1$ or $q = 1$), we have the following additional result [48].

Proposition 2. *Suppose that* $\operatorname{rank}(C) = 1$ *so that there exists* $v, w \in \mathbb{R}^m$ *with* $C = vw^T$. *If* $\operatorname{rank}([v, Bv, \ldots, B^{p-1}v]) = \operatorname{rank}([w, B^T w, \ldots, (B^{p-1})^T w]) = p$, *then there is a one-to-one mapping between* $\mathcal{S}_J$ *and* $\mathcal{S}_{\mathcal{L}^+}$. *Moreover,*

$$Sp(\mathcal{L}) = \{0\} \cup \left\{ 1/w^T (B - \mu I_n)^{-1} v,\ \mu \in Sp(J) \setminus Sp(B) \right\}.$$

6 PDEs on metric graphs

The notion of metric graph was introduced in Subsection 3.2. In the current section we are going to investigate dynamic processes defined on this kind of structures.

6.1 Hyperbolic equation on networks

The simplest hyperbolic equation models the advection or transport process on an interval. We consider it along the arcs of a metric graph $\mathcal{G}$. For simplicity, we rescale all edge lengths to 1. On the edge e_j, which we parametrise as $[0, 1]$, we take the equation

$$\frac{\partial}{\partial t} u_j(t, s) = c_j \cdot \frac{\partial}{\partial s} u_j(t, s), \quad t > 0,\ s \in (0, 1), \quad j \in J, \tag{16}$$

where the velocity coefficients are $c_j > 0$ for all $j \in J$ and the flow is assumed to move in the direction opposite to the parametrisation, i.e., from endpoint 1 to endpoint 0. Let us remark that one could also consider space- or time-variable coefficients c_j, as was done in [21, 24, 47] or [10], respectively. Denote

$$C := \operatorname{diag}(c_j).$$

For the well-posedness of our problem, we should impose boundary conditions at the right endpoint of every edge, i.e., at 1. We shall assume that the weights w_j on the edges of the underlying weighted combinatorial digraph G (see Subsection 3.1) satisfy

$$0 < w_j \leq 1 \quad \text{and} \quad \sum_{e_j \in E^-_{v_i}} w_j = 1, \tag{17}$$

for all $j \in J$ and $v_i \in V$. In particular, for the weighted outgoing degree matrix, we have $\mathcal{D}^-_w = I_n$. The standard boundary conditions for our problem can be written as

$$c_j u_j(t, 1) = w_j \left[\Phi^+ C u(t, 0) \right]_i \tag{18}$$

for every edge $e_j \in E^-_{v_i}$. We assume without loss of generality that G has no sinks or sources (see also [4, Thm. 2.1]). Here and further on,

$$u(t, s) = (u_j(t, s))_{j \in J}$$

denotes the vector of function(value)s on the edges.

Note, that (17) guarantees the conservation of mass in every vertex and that conditions (17)–(18) imply so-called *Kirchhoff's law* that can be formulated in terms of incidence matrices as

$$\Phi^- Cu(t,1) = \Phi^+ Cu(t,0). \tag{19}$$

The following result was proved in [40, Prop. 2.5] and [7, Prop. 18.15].

Proposition 3. *Let G be a finite connected digraph with no sinks or sources, given by the incidence matrices Φ^- and Φ^+, and consider the system on the arch of the corresponding metric graph $\mathcal{G}$,*

$$\begin{cases} \frac{\partial}{\partial t} u_j(t,s) &= c_j \cdot \frac{\partial}{\partial s} u_j(t,s), & t>0,\ s\in(0,1), \\ \phi_{ij}^- c_j u_j(t,1) &= w_{ij} \sum_{k\in J} \phi_{ik}^+ c_k u_k(t,0), & t>0, \\ u_j(0,s) &= f_j(s), & s\in[0,1]\,, \end{cases} \tag{20}$$

with coefficients $c_j > 0$ and w_j satisfying (17), for $j \in J$, $i \in I$. Then the problem is well-posed on the space $L^1\big([0,1],\mathbb{C}^m\big)$. The solution to (20) is given by

$$u_f(t) = T(t)f, \quad t \geq 0,$$

where $(T(t))_{t\geq 0}$ is a C_0-semigroup on $L^1\big([0,1],\mathbb{C}^m\big)$ and $u_f(t) = u_f(t,\cdot)$ denotes the vector of solution functions on the edges with initial value f.

Remark 1. *The same result was in [47, Prop. 2.3] and [21, Cor. 2.19] obtained also for non-constant coefficients c_j.*

Moreover, problem (20) is well-posed also on $L^p\big([0,1],\mathbb{C}^m\big)$ for $1 \leq p < +\infty$, see [21, Cor. 2.19] and [24, Prop. 3.1].

The generator of the semigroup $(T(t))_{t\geq 0}$ in the above proposition is the operator defined as

$$A_F := C \cdot \frac{d}{ds}, \quad D\left(A_F\right) := \left\{ f \in \mathrm{W}^{1,1}\big([0,1],\mathbb{C}^m\big) \colon f(1) = \mathcal{B}_C^+ f(0) \right\} \tag{21}$$

(for the condition of the domain see [7, Prop. 18.2]), where where $\mathcal{B}_C^+$ is the weighted adjacency matrix of the line graph obtained as

$$\mathcal{B}_C^+ := C^{-1} \mathcal{B}_w^+ C.$$

Under the assumption on the weights (17), the matrix $\mathcal{B}_w^+$ is column stochastic. This turns out to be important when studying further qualitative properties of the solutions. Many properties of the solution semigroup are given by the structure of the graph. For example, the semigroup $(T(t))_{t\geq 0}$ is irreducible if and only if the oriented graph G is strongly connected (cf. [7, Prop. 18.16] and [47, Lem. 4.5]).

The spectrum of the operator $(A_F, D(A_F))$ can be characterized using the weighted adjacency matrix $\mathcal{A}_w^+$, the weighted adjacency matrix of the line graph $\mathcal{B}_C^+$ or, equivalently, the advection matrix $\mathcal{N}_w^+$ as follows. We start by adjusting the nonzero coefficients of these matrices. Define

$$E_\lambda(s) := \operatorname{diag}\left(e^{\frac{\lambda}{c_k} s}\right), \quad s \in \mathbb{R}, \tag{22}$$

and let

$$\mathcal{A}_\lambda^+ := \Phi^+ E_\lambda(-1)\left(\Phi_w^-\right)^\top, \quad \mathcal{B}_{C,\lambda}^+ := E_\lambda(-1)\mathcal{B}_C^+, \quad \text{and} \quad \mathcal{N}_\lambda^+ := I - \mathcal{A}_\lambda^+.$$

Notice that $\mathcal{A}_0^+ = \mathcal{A}_w^+$, $\mathcal{B}_{C,0}^+ = \mathcal{B}_C^+$, and $\mathcal{N}_0^+ = \mathcal{N}_w^+$ (recall that $\mathcal{D}_w^- = I_n$ by (17)).

Theorem 1. *Let $(A_F, D(A_F))$ be the operator given in* (21)*. Then*

$$\lambda \in \sigma(A_F) = \sigma_p(A_F) \Longleftrightarrow 1 \in \sigma(\mathcal{A}_\lambda^+) \Longleftrightarrow 1 \in \sigma(\mathcal{B}_{C,\lambda}^+) \Longleftrightarrow 0 \in \sigma(\mathcal{N}_\lambda^+).$$

Moreover, g is an eigenfunction of A_F corresponding to the eigenvalue λ if and only if $g(s) = E_\lambda(s)d$ where d is an eigenvector of $\mathcal{B}_{C,\lambda}$ corresponding to the eigenvalue 1.

Proof. The equalities about the spectra follow from the explicit formula of the resolvent $R(\lambda, A_F)$ which is positive and compact, see [7, Cor. 18.13]. Observe that the eigenspace $\ker(\lambda - A_F)$ is spanned by the functions of the form $g(\cdot) = E_\lambda(\cdot)d$ for some $d \in \mathbb{C}^J$ such that $g(1) = \mathcal{B}_C^+ g(0)$. The given correspondence between eigenvectors can be derived by an easy calculation. □

The following condition plays a crucial role in the long-term behaviour of the solutions.

$$\begin{gathered}\text{There exists } 0 < d \in \mathbb{R} \text{ such that } d \cdot \left(\frac{1}{c_{j_1}} + \cdots + \frac{1}{c_{j_k}}\right) \in \mathbb{N} \\ \text{for all directed cycles } e_{j_1}, \ldots, e_{j_k} \text{ in } G.\end{gathered} \tag{23}$$

If (23) is satisfied, the boundary spectrum of A_F is cyclic (see [7, Prop. 18.1b]). Moreover, in this case also a so-called *circular spectral mapping theorem* holds for the spectrum of the generator $(A_F, D(A_F))$ and the semigroup $(T(t))_{t\geq 0}$, see [40, Prop. 3.8] and [47, Prop. 4.10]. This states the following:

$$\Gamma \cdot e^{t\sigma(A_F)} = \Gamma \cdot \sigma(T(t)) \setminus \{0\} \text{ for each } t \geq 0,$$

where Γ denotes the unit circle.

From the spectral properties of the generator we can obtain the asymptotic behavior of the solutions of the problem (20), see [40, Thm. 4.10] and [7, Thm. 18.19]. We call a subgraph G_r of G a *terminal strong component* if it is strongly connected and there are no outgoing edges of G_r, see [5, page 17].

Theorem 2. *Let G be a connected graph with terminal strong components $G_1, \ldots, G_\ell$ and $(T(t))_{t\geq 0}$ the semigroup associated with the transport problem* (20)*. Then for any initial value $f \in L^1\big([0,1], \mathbb{C}^m\big)$ the (mild) solution of system* (20) *can be written uniquely in the form of a sum*

$$\begin{aligned} u_f(t) = T(t)f &= T_n(t)f + T_s(t)f + T_{r_1}(t)f + \cdots + T_{r_\ell}(t)f, \\ &\coloneqq u_{n,f}(t) + u_{s,f}(t) + u_{r_1,f}(t) + \cdots + u_{r_\ell,f}(t), \quad t \geq 0, \end{aligned}$$

where $T_n(\bullet)$, $T_s(\bullet)$, $T_{r_1}(\bullet)$, $\ldots$, $T_{r_\ell}(\bullet)$ are strongly continuous semigroups on the $T(t)$-invariant subspaces X_n, X_s, X_{r_1}, $\cdots$, X_{r_ℓ}, respectively, with

$$L^1\big([0,1], \mathbb{C}^m\big) = X_n \oplus X_s \oplus X_{r_1} \oplus \cdots \oplus X_{r_\ell},$$

and the following holds.

1. *There exists* $t_0 > 0$ *such that* $u_{n,f}(t) = 0$ *for all* $t \geq t_0$.
2. *The solution on* X_s *is stable:* $\lim\limits_{t\to+\infty} u_{s,f}(t) = 0$.
3. *If for some* $1 \leq i \leq \ell$ *the graph* G_i *satisfies Condition* (23) *then for the period*

$$\tau_i = \frac{1}{d}\gcd\left\{d\cdot\left(\frac{1}{c_{j_1}}+\cdots+\frac{1}{c_{j_k}}\right) : e_{j_1},\dots,e_{j_k} \text{ is a directed cycle in } G_i\right\},$$

the solution on X_{r_i} *behaves periodically:*

$$u_{r_i,f}(t+\tau_i) = u_{r_i,f}(t), \quad t \in \mathbb{R}.$$

4. *If for some* $1 \leq i \leq \ell$ *graph* G_i *does not satisfy Condition* (23)*, then for the solution on* X_{r_i} *it holds*

$$\lim_{t\to+\infty} u_{r_i,f}(t) = \mathcal{P}_{X_{r_i}} f,$$

where $\mathcal{P}_{X_{r_i}}$ *denotes the projection onto the one-dimensional subspace* X_{r_i}.

Therefore, the structure of the discrete graph strongly influences the long-term behavior of the solutions to the given problem.

Let us also note that one can generalize the problem and consider a system of hyperbolic equations on each graph edge. Such problems were studied in [23] in the L^2-setting where the existence of the solutions was obtained under appropriate assumptions for the (not necessarily hermitian) coefficient matrices and admissible boundary conditions.

We further mention that stabilization results of some hyperbolic systems on graphs are available in [54, 32], where exponential or polynomial energy decay is obtained.

Another class of problem (20) generalizations' is transport on time-varying metric graphs. Depending on the types of graph modifications one can mention: [8] where time-dependent weights are considered, [10] with both weights and velocities of flow differing in time, and finally [46] where not only coefficients but also the structure itself can be modified.

6.2 Virus variant modeling in fragmented environment

Let us now return to the question of how to describe the evolution of variants of the virus in the diverse environment, presented in motivating example 2.7.

We consider P patches that can be interpreted either as cities or larger areas divided by natural barriers such as rivers, mountain ranges etc., and enumerated by $J_p = \{1,\dots,P\}$. In each patch there are $Q-1$ variants of a virus, having its specific virus infection average duration t_q, $q \in J_q = \{1,\dots,Q-1\}$, and uncolonised persons with reference time t_Q when their status of colonisation remain unchanged. In order to structure

this topography into the metric graph, consider two kinds of edges e_j, $j \in J_V$ or $j \in J_{nV}$ $J = J_V \cup J_{nV}$, $\#J = m$, where

$$\begin{aligned} J_V &:= \{(p-1)Q+q : \ p \in J_p, \ q \in J_q\}, \\ J_{nV} &:= \{pQ : \ p \in J_p\}. \end{aligned}$$

In particular, the flow along the edge $e_{(p-1)Q+q}$, for $p \in J_p, q \in J_q$, describes the evolution of infection of q-th virus in p-th patch from the moment of contamination at $e_{(p-1)Q+q}(1)$ to patients' recovery in $e_{(p-1)Q+q}(0)$. The evolution of the population of uncolonised persons in p-th patch, in time, is related with the flow on the edge e_{pQ}, $p \in J_p$.

The velocities of flow, for above types of edges, respectively for $q \in J_q$ and $p \in J_p$, are given by

$$c_{(p-1)Q+q} = t_q^{-1}, \quad c_{pQ} = t_Q^{-1}.$$

Due to the inaccuracy of parameter estimation, we can assume without loss of generality that all $t_j \in \mathbb{Q}_+$, $j \in J$ and consequently (23) always holds.

The mobility of modeled society as well as virus mutations are described by the entries of $\mathcal{B} = (b_{ij})_{i,j\in J}$ that inform about the fraction of people changing their status of colonisation in different patches. Namely, entry $b_{(p-1)Q+q_1,(p-1)Q+q_2}$, $p \in J_p, q_1, q_2 \in J_q$ gives the intensity of mutation from q_2-th variant to q_1-th variant of virus in patch p, while $b_{(p_1-1)Q+q,(p_2-1)Q+q}$, $p_1, p_2 \in J_p, q \in J_q$ the intensity of transfer of patients colonised by q-th variant of a virus from patch p_2 to p_1. Furthermore $b_{(p-1)Q+q,(p-1)Q+q}$, $p \in J_p, q \in J_q$ gives the intensity of infections that last longer then average time t_q in patch p. We assume additionally that

$$b_{(p_1-1)Q+q_1,(p_2-1)Q+q_2} = 0, \quad \text{for } p_1 \neq p_2, q_1 \neq q_2, \ p_1, p_2 \in J_p, q_1, q_2 \in J_q$$

hence the mutations appear only in patches.

Entry $b_{(p-1)Q+q,pQ}$, $p \in J_p, q \in J_q$, informs about the intensity of colonisation of uncolonised persons by q-th variant of a virus in patch p. We assume that

$$b_{(p_1-1)Q+q,p_2Q} = 0 \quad \text{for } p_1 \neq p_2, \ p_1, p_2 \in J_p, q \in J_q$$

hence the colonisation appears in the patch only.

Analogously, $b_{pQ,Q(p-1)+q}$, $p \in J_p, q \in J_q$ is related to the intensity of recovery of infected persons colonised by q-th variant of a virus in patch p. Additionally,

$$b_{p_2Q,Q(p_1-1)+q} = 0 \quad \text{for } p_1 \neq p_2, p_1, p_2 \in J_p, \ q \in J_q$$

hence the recovery appears in the patch.

Finally, b_{p_1Q,p_2Q}, $p_1, p_2 \in J_p$ is the intensity of transfer of uncolonised persons from p_2-nd patch to p_1-st patch.

Now based on Thm. 2 we estimate the influence of a particular variant of a virus in the considered patch. If an edge $e_{(p-1)Q+q}$, $p \in J_p$, $q \in J_q$ does not belong to any terminal strong component G_r we have two possible scenarios. Either q-th variant of a virus will extinct in p patch in

a predictable time horizon. For that, the $(p-1)Q+q$-th coordinate has to vanish everywhere except from X_s subspace. Otherwise variant q will be vanishing gradually from patch p and its influence on the population will be negligible. Consequently, in both presented cases variant q should not be taken into account for vaccination policies in patch p.

Now, let us consider an edge $e_{(p-1)Q+q}$, $p \in J_p, q \in J_q$ that belongs to a terminal strong component G_r. We denote edges of G_r by

$$E^r := \{e_{(p-1)Q+q} : p \in J_p{}^r,\ q \in J_q{}^r(p)\} \cup \{e_{pQ} : p \in J_p{}^{r'}\},$$

$J_p{}^r, J_p{}^{r'} \subset J_p$, $J_q(p) \subset J_q$. By the definition, there is only one terminal strong component that $e_{(p-1)Q+q}$ belongs to but coordinate $(p-1)Q+q$ may not vanish on subspaces X_n, X_s. The subgraph G_r identifies $p^r := \#J_p{}^r$ connected patches in which $q^r := \#Q^r$, $Q^r := \{q \in J_q{}^r(p) :\ p \in J_p{}^r\}$, variants of virus play a role. In the long therm flow of a virus between those patches is periodic hence one can compute the average number of patients colonised by q-th variant of a virus in r-th terminal strong component. Consider initial distribution of patients in patches f and define a mean $\Pi^r : L^1\big([0,1], \mathbb{C}^m\big) \to \mathbb{R}^m$

$$\Pi^r f = \frac{1}{\tau_r} \int_0^{\tau_r} \int_0^1 (T_r(s)f)(x) dx ds, \quad \text{for any } t \geq 0.$$

One can compute the proportion of patients being colonised by a particular variant of a virus in the patch. For fixed patch p consider strong components G_{r_i}, $i = 1, \ldots, \ell$, such that for each of them there exist an edge $e_{(p-1)Q+q}$, $q \in J_q^{r_i}$, $i = 1, \ldots, \ell$. The vector of averaged prevalence $\mathrm{Prev}(p) = (\mathrm{Prev}_q(p))_{q \in J_q}$ in p-th patch is given by

$$\mathrm{Prev}_q(p) := \frac{(\sum_{i=1}^{\ell} \Pi^{r_i} f)\, \mathbf{e}_{(p-1)Q+q}}{(\sum_{i=1}^{\ell} \Pi^{r_i} f)\, \mathbb{1}}, \quad q \in J_q,$$

where $\mathbb{1}$ is defined in (11) and $e_{(p-1)Q+q} = (0, \ldots, 0, 1, 0 \ldots, 0)^T \in \mathbb{R}^m$. Based on this the prevalence $\mathrm{Prev}(p)$ medical authorities can make appropriate assignment of vaccine in the patch p.

6.3 Laplace equation on graphs

We shall now move to second order problems and consider diffusion process on an interval along the arcs of a metric graph $\mathcal{G}$. We adopt the following notation for function u_j, defined on the edge e_j, parameterized on $[0,1]$:

$$u_j(v_i) = \begin{cases} u_j(0) & \text{if } v_i \overset{e_j}{\to}, \\ u_j(1) & \text{if } \overset{e_j}{\to} v_i. \end{cases} \qquad \frac{d}{ds} u_j(v_i) = \begin{cases} \frac{d}{ds} u_j(0) & \text{if } v_i \overset{e_j}{\to}, \\ \frac{d}{ds} u_j(1) & \text{if } \overset{e_j}{\to} v_i, \end{cases}$$

if, in the latter case, the (one-sided) derivatives exist. Let us first recall the definition of the (continuous) Laplacian $\Delta_{\mathcal{G}}$ on a metric graph $\mathcal{G}$ with Kirchhoff boundary condition at the vertices. In the following, $C(\mathcal{G})$ denotes the space of continuous functions on the edges being continuous across the vertices, that is,

$$C(\mathcal{G}) := \{u = (u_j)_{j \in J} \in \prod_{j \in J} C[0,1] : u_j(v_i) = u_k(v_i) \text{ if } \phi_{ij}\phi_{ik} \neq 0\},$$

where

$$\Phi = (\phi_{ij})_{i\in I, j\in J} = \Phi^+ - \Phi^-$$

denotes the incidence matrix of the underlying graph G. Let

$$D(\Delta_{\mathcal{G}}) := \{u \in C(\mathcal{G}) : u_j \in H^2(0,1), \forall j \in J, \sum_{l\in J} \phi_{il} \frac{d}{ds} u_l(v_i) = 0, \forall i \in I\} \tag{24}$$

and

$$\Delta_{\mathcal{G}} u := \left(-\frac{d^2}{ds^2} u_j\right)_{j\in J}. \tag{25}$$

It is not difficult to show that $\Delta_{\mathcal{G}}$ is a non-negative self-adjoint operator with a compact resolvent.

In the same spirit as the result from Theorem 1 from Subsection 6.1, let us recall an old result from [66, 53] concerning the relationship between the spectrum of the operator $\Delta_{\mathcal{G}}$ when the lengths of the edges are all equal to 1 with the eigenvalues of a matrix. Let

$$\widetilde{\mathcal{A}} := \mathcal{D}^{-1}\mathcal{A}$$

which is also called the transition matrix of G, where $\mathcal{A}$ is the adjacency matrix of G, see (4), and $\mathcal{D}$ is the degree matrix of G, see (5).

Theorem 3. *Assume that the lengths of the edges of the metric graph $\mathcal{G}$ are all equal to 1. Then the spectrum $\sigma(\Delta_{\mathcal{G}})$ consists only of eigenvalues and is given by*

$$\sigma(\Delta_{\mathcal{G}}) = S_1 \cup S_2,$$

where

$$S_1 = \{\pi^2 k^2 : k \in \mathbb{N}\},$$

the multiplicity of 0 is 1, while the multiplicity of $\pi^2 k^2$ depends on the fact of whether G is bipartite or not. Furthermore,

$$S_2 = \{\lambda \in (0,\infty) : \cos\sqrt{\lambda} \in \sigma(\widetilde{\mathcal{A}}) \cap (-1,1)\}.$$

Let us notice that the main idea for the characterization of the family S_2 is to look for an eigenvector u in the form

$$u_j(s) = \frac{u_j(0)\sin(\sqrt{\lambda}(1-s)) + u_j(1)\sin(\sqrt{\lambda}s)}{\sin\sqrt{\lambda}}, \quad s \in [0,1],$$

which is meaningful since $\sin\sqrt{\lambda} \neq 0$. By the continuity condition at the vertices, the remaining unknowns are the values of u at the vertices and we easily check that the Kirchhoff conditions at the nodes lead to

$$\widetilde{\mathcal{A}} X = \cos\sqrt{\lambda} X,$$

where

$$X = (u(v))_{v\in V} \tag{26}$$

denotes the vertex values of u which are well-defined for a function $u \in C(\mathcal{G})$.

This method gives also an explicit relationship between the eigenvector u of $\Delta_{\mathcal{G}}$ associated with λ and the eigenvector X of $\widetilde{\mathcal{A}}$ associated with $\cos\sqrt{\lambda}$.

In the following, we consider a diffusion problem on $\mathcal{G}$ of the form

$$\begin{cases} \frac{\partial}{\partial t}u_j(t,s) &= \frac{\partial^2}{\partial s^2}u_j(t,s), & t>0,\ s\in(0,1),\\ u_j(v_i) &= u_k(v_i) & \text{if } \phi_{ij}\phi_{ik}\neq 0,\\ 0 &= \sum_{l\in J}\phi_{il}\frac{d}{ds}u_l(t,v_i), & t>0,\\ u_j(0,s) &= f_j(s), & s\in[0,1]\,, \end{cases} \tag{27}$$

where $j,k\in J$, $i\in I$. It can be easily seen that the above system is equivalent to the abstract Cauchy problem

$$\begin{cases} \frac{d}{dt}u(t) = -\Delta_{p,\mathcal{G}}u,\\ u(0)=f, \end{cases} \tag{28}$$

with state space $L^p\big([0,1],\mathbb{C}^m\big)$, where

$$\begin{aligned} D(\Delta_{p,\mathcal{G}}) = \{u\in C(\mathcal{G}):\quad & u_j\in W^{2,p}(0,1),\ \forall j\in J\\ & \text{and } \textstyle\sum_{l\in J}\phi_{il}\frac{d}{ds}u_l(v_i)=0,\ \forall i\in I\big\} \end{aligned} \tag{29}$$

and

$$\Delta_{p,\mathcal{G}}u = \left(-\frac{d^2}{ds^2}u_j\right)_{j\in J}. \tag{30}$$

In [25, Thm. 3.6], the following result is shown, see also [20, Cor. 2.13] and [24, Prop. 3.3].

Theorem 4. *The first-order problem* (28) *is well-posed on the space* $L^p\big([0,1],\mathbb{C}^m\big)$ *for* $1\le p<+\infty$, *i.e., for all initial data* $f\in L^p\big([0,1],\mathbb{C}^m\big)$ *problem* (28) *admits a unique mild solution that continuously depends on the initial data. The solutions on the appropriate spaces have the form*

$$u_{p,f}(t) = T_p(t)f,\quad t\ge 0, \tag{31}$$

where $(T_p(t))_{t\ge 0}$ *is the* C_0*-semigroup generated by* $-\Delta_{p,\mathcal{G}}$ *on* $L^p\big([0,1],\mathbb{C}^m\big)$.

By [25, Cor. 5.2], we can also describe the asymptotic behavior of the solutions to (28).

Theorem 5. *Let* $f\in L^p\big([0,1],\mathbb{C}^m\big)$, $1\le p<+\infty$, *be arbitrary. For the solutions of the problem* (28) *with initial value* f *the following hold.*

1. *The limit* $\lim\limits_{t\to+\infty}u_{p,f}(t)=\mathcal{P}f$ *exists.*
2. $\mathcal{P}$ *is the strictly positive projection onto the one-dimensional subspace of* $L^p\big([0,1],\mathbb{C}^m\big)$ *spanned by the constant function* 1, *which is the kernel of* $\Delta_{p,\mathcal{G}}$.
3. *For every* $\varepsilon>0$ *there exists* $M>0$ *such that*

$$\|u_{p,f}(t)-\mathcal{P}f\|\le M\mathrm{e}^{\varepsilon+\lambda_2 t},$$

where λ_2 *is the largest nonzero eigenvalue of* $\Delta_{\mathcal{G}}$.

In [39] we perturbed the Kirchhoff boundary condition of the diffusion problem (27) in each vertex by noise, that is, we considered the system

$$\begin{cases} \frac{\partial}{\partial t}u_j(t,s) &= \frac{\partial^2}{\partial s^2}u_j(t,s), & t>0,\ s\in(0,1),\\ u_j(v_i) &= u_k(v_i) & \text{if } \phi_{ij}\phi_{ik}\neq 0,\\ \dot\beta_{v_i}(t) &= \sum_{l\in J}\phi_{il}\frac{d}{ds}u_l(t,v_i), & t\in(0,T],\\ u_j(0,s) &= f_j(s), & s\in(0,1)\,, \end{cases} \tag{32}$$

where $j, k \in J$, $i \in I$ and

$$(\beta(t))_{t\in[0,T]} = \Big((\beta_{v_i}(t))_{t\in[0,T]}\Big)_{i\in I},$$

is an $\mathbb{R}^n$-valued Brownian motion (Wiener process) on an appropriate complete probability space. For an initial function $f \in L^2\big([0,1],\mathbb{C}^m\big)$, the mild solution of problem (32) has the form

$$\tilde{u}_f(t) = u_{2,f}(t) + \int_0^t (\lambda + \Delta_{\mathcal{G}})S(t-s)D_\lambda \, d\beta(s), \quad t \geq 0, \tag{33}$$

where $u_{2,f}$ is the solution of the diffusion problem on L^2 from (31), $\lambda > 0$ is arbitrary, and D_λ is the so-called Dirichlet-operator. In [39, Thm. 3.8] we showed the following result.

Theorem 6. *Let (f_k) be the complete orthonormal system consisting of the eigenfunctions of $\Delta_{\mathcal{G}}$ in $L^2\big([0,1],\mathbb{C}^m\big)$, and assume that there exists a positive constant c such that*

$$\sup\{|f_k(v)| : v \in V,\, k \in \mathbb{N}\} \leq c.$$

Then, for $\alpha < \frac{1}{4}$ the mild solution $\tilde{u}_f$ has a continuous version in the fractional domain space $D\left(\Delta_{\mathcal{G}}^{\alpha}\right)$.

7 PDEs on embedded metric graphs

7.1 Traffic analysis

An example of application of metric graphs that are embedded into the plane are traffic models, in particular macroscopic ones, which are usually based on partial differential equations describing the evolution of aggregated values such as traffic density, traffic flow and average speed. In our work, we have focused on one of the popular macroscopic traffic simulation models, the Payne-Whitham model [63, 68], originally designed for modelling highway traffic on straight road segments. Our model is derived from the one in [38], the main novelty being that we considered that some of the road segments are controlled by traffic signals. In particular, we focused on how drivers react to the change of state of a traffic light and improved the model from [38] by taking into account a speed reduction when cars enter a junction and turn left or right.

The Payne-Whitham model on a single edge (i.e. road segment) consists of a conservation law for density, together with a characterisation of the instantaneous variation of speed based on the behaviour of drivers in terms of their adaptation to the current density and also their ability to anticipate the changes in density upstream. The equations are the following:

$$\frac{\partial \rho(t,x)}{\partial t} + \frac{\partial (v(t,x)\rho(t,x))}{\partial x} = 0 \tag{34}$$

$$\frac{\partial v(t,x)}{\partial t} + v(t,x)\frac{\partial (v(t,x))}{\partial x} = \frac{V(\rho(t,x)) - v(t,x)}{\nu} - \frac{C}{\rho(t,x)}\frac{\partial \rho(t,x)}{\partial x}, \tag{35}$$

where the function V represents the ideal relationship between density and speed on a road segment (called the "fundamental diagram of traffic flow"). In our work, it has the following form:

$$V(\rho) = v_{max} \exp\left(-\frac{1}{a}\left(\frac{\rho}{\rho_{cr}}\right)^a\right), \tag{36}$$

where v_{max} (the maximum speed), ρ_{cr} (the density where the speed starts to decrease considerably) and a (characterising the steepness of this decrease) are positive parameters inherent to every edge of the road network (see [12, Section 2.1] for more details). The meaning of the conservation law (34) is that the density of cars propagates with the speed given by $v(t, x)$. Similarly, the speed also propagates with the traffic flow, but its variation also depends on other factors given on the right-hand side (RHS) of (35). In particular, the first term on the RHS of (35) drives the speed towards the ideal speed given by the fundamental diagram (36). The strength of this adaptive behaviour is controlled by the parameter $\nu > 0$, which must be calibrated to describe the real-world situation of interest. The second term on the RHS of (35) represents the ability of drivers to anticipate the traffic conditions ahead and adapt their speed to the change in density. The strength of this ability to anticipate is described by the parameter $C > 0$.

Next, we use an explicit finite difference scheme to compute the density and speed at the next time step $k + 1$ with respect to the current state (at time step k) for each road e uniformly discretised into N_e segments indexed by $i \in \{1, 2, \ldots, N_e\}$ (where vehicles travel from the segment $i-1$ directly to the segment i):

$$\frac{\rho(k+1,i) - \rho(k,i)}{\delta t} + \frac{\rho(k,i)v(k,i) - \rho(k,i-1)v(k,i-1)}{\delta x} = 0; \tag{37}$$

$$\begin{aligned} &\frac{v(k+1,i) - v(k,i)}{\delta t} + \frac{v(k,i)^2 - v(k,i-1)^2}{2\delta x} \\ &\quad = \frac{V(\rho(k,i+1)) - v(k,i)}{\nu} - \frac{C}{\rho(k,i) + \chi}\frac{\rho(k,i+1) - \rho(k,i)}{\delta x}. \end{aligned} \tag{38}$$

Here δt and δx are the discretisation grid sizes and $\chi > 0$ is a parameter used to avoid blow-ups in the last term of (38). It may also need to be calibrated to reflect the local situation. We refer to [12, Section 3] for more details about discretisation technique and the stability conditions for (37)-(38).

7.1.1 Coupling at intersections

In the case of a road network, the number of lanes on each street might differ and the cars need to adapt to the lane number change by modifying the speed. Therefore, the network version of the Payne-Whitham model should take into account the number of lanes $\ell(e)$ corresponding to each edge e of the graph. The next step is to write the equation (37) in terms

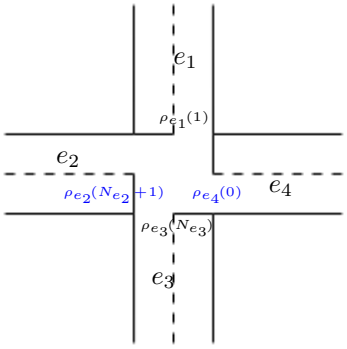

Figure 3: An intersection with the virtual initial and final densities (blue values are virtual).

of the traffic flux (i.e. the number of cars passing on all lanes in each instant of time):

$$q(k,i) = \rho(k,i)v(k,i)\ell(e). \tag{39}$$

where $\rho(k,i)$ is the density per lane averaged over all lanes. Therefore, the equation (37) can be written as:

$$\frac{\rho(k+1,i)-\rho(k,i)}{\delta t} + \frac{1}{\ell(e)}\frac{q(k,i)-q(k,i-1)}{\delta x} = 0. \tag{40}$$

Further, it can be observed that some quantities needed to perform the iteration in (40) and (38) are not available from the previous time step. Namely, in order to compute the density and speed for both ends of a road segment e (parameterised by $\{1,2,\ldots,N_e\}$), we need some virtual values for $q(k,0)$, $\rho(k,N_e+1)$ and $v(k,0)$.

In the case of no traffic lights, we follow the ideas in [38, Section II.D], where these virtual values are defined as weighted sums of the traffic values on the other road segments adjacent to this intersection. We illustrate these calculations for the particular case of the intersection in Figure 3:

$$q_{e_4}(k,0) = \sum_{i=1}^{4} q_{e_i}(k,N_{e_i}) \cdot \frac{\omega(e_i,e_4)}{\sum_{j=1}^{4}\omega(e_i,e_j)}; \tag{41}$$

$$v_{e_4}(k,0) = \frac{1}{q_{e,4}(k,0)} \sum_{i=1}^{4} v_{e_i}(k,N_{e_i}) \cdot q_{e_i}(k,N_{e_i}) \cdot \frac{\omega(e_i,e_4)}{\sum_{j=1}^{4}\omega(e_i,e_j)}. \tag{42}$$

A similar approach is employed to calculate $\rho_{e_2}(k,N_{e_2}+1)$ (see [12, Section 4.1]). The turning weights $\omega(e_i,e_j)$ represent the number of cars that choose to continue their trip on road e_j, after entering that particular intersection from road e_i. These weights are determined by processing real-world traffic data.

7.1.2 Limiting the turning speed

Our first improvement to the algorithm in [38] concerns the maximum speed of cars changing direction at an intersection. We have limited the virtual initial speed $v(k,0)$ according to the speed at the other edges in the intersection and the geometry of the intersection. We illustrate the procedure using the notation in Figure 3:

$$v_{e_4}^{lim}(k,0) = \frac{1}{q_{e_4}(k,0)} \sum_{i=1}^{4} v_{e_i}^{max} \frac{(1-\cos(\widehat{e_i,e_4}))}{2} q_{e_i}(k,N_{e_i}) \cdot \frac{\omega(e_i,e_4)}{\sum_{j=1}^{4}\omega(e_i,e_j)}, \tag{43}$$

where $v_{e_i}^{max}$ is the speed at which cars normally travel when the road is empty. See [12, Section 4.2] for more details about this way of limiting speed at intersections.

7.1.3 Adding traffic lights

Our major contribution to the traffic simulation model is introducing traffic signal control for some intersections. The modifications imply both the speed values at the end of the roads controlled by traffic lights and the weighted sums (41)-(43). If the signal is red, the final speed $v(N_e)$ of the edge e is set to 0 and e is not taken as an input in the weighted sums for the virtual density and speed of other edges (i.e., we set $\omega(e,e_i)=0$ for each road e_i).

7.2 Approximating PDEs on $\mathbb{R}^2$ with equations on embedded graphs

Another application of embedded graphs lies in their capability to approximate solutions of PDEs in a two-dimensional space using a coupled system of one-dimensional equations on a grid contained within $\mathbb{R}^2$. In this context, we highlight the results in [9] on the Dirichlet problem in the square $\mathcal{S} = (0,1)\times(0,1)$

$$\begin{cases} -\Delta u = f, & \text{on } \mathcal{S}; \\ u = 0, & \text{on } \partial\mathcal{S}, \end{cases} \tag{44}$$

where f is a continuous function on $\overline{\mathcal{S}}$.

In order to approximate the solution of the above problem, we consider the traditional equidistant grid in the square, but now seen as a metric graph $\mathcal{G}$. Namely, for any N a positive integer ($N \geq 3$), we set the grid width $h = 1/N$ and the digraph $G_h = (V_h, E_h, \Phi_h^{\pm}, W_h)$, defined as follows (see Figure 4):

The set of vertices

$$\begin{aligned} V_h &:= \left\{ v_i = \left(v_i^1, v_i^2\right) : i \in I^h \right\} \\ &:= \{(kh, jh) : k,j \in \mathbb{N} \cap [0,N] \text{ not both belonging to } \{0,N\}\} \end{aligned}$$

gets divided into two components, the set of internal and boundary vertices, respectively:

$$V_h^{ext} \coloneqq \left\{v \in V_h : \ v^1 \in \{0, N\} \text{ or } v^2 \in \{0, N\}\right\};$$
$$V_h^{int} \coloneqq V_h \setminus V_h^{ext}.$$

The edges connect every two adjacent (in the sense of coordinate number) vertices that are not both exterior nodes, namely

$$\begin{aligned} E_h &\coloneqq \left\{e_j : j \in J^h\right\} \\ &\coloneqq \left\{(v_i, v_k) : \ \left|v_i^1 - v_k^1\right| + \left|v_i^2 - v_k^2\right| = 1, \text{ and } v_i \text{ or } v_k \in V_h^{int}\right\}. \end{aligned}$$

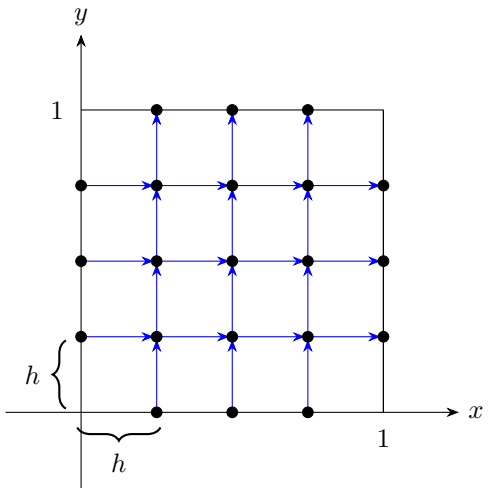

Figure 4: The discretisation of the square $\mathcal{S} \subset \mathbb{R}^2$. The edges of the graph G_h are coloured in blue.

In order to obtain a metric graph $\mathcal{G}_h$ we add the orientation to G_h which agrees with the positive direction of each axis (see Figure 4). Furthermore, we assume that digraph is unweighted, hence W_h is an identity matrix. This allows us to consider the Dirichlet problem on $\mathcal{G}_h$ corresponding to the Kirchhoff Laplacian $\Delta_{\mathcal{G}_h}$ defined in Subsection 6.3, with Dirichlet boundary conditions at the exterior vertices that are now part of the operator domain:

$$\begin{aligned} D\left(\Delta_{\mathcal{G}_h}\right) = \Big\{ & u = (u_j)_{j \in J^h} \in C(\mathcal{G}_h) : u_j \in H^2(e_j), \, \forall e_j \in E_h, \\ & \sum_{j \in J^h} \left(\phi_{h,ij}^+ - \phi_{h,ij}^-\right) u_j'\left(v_i\right) = 0, \, \forall v_i \in V_h^{int} \text{ and} \\ & u(v_i) = 0, \, \forall v_i \in V_h^{ext} \Big\} \end{aligned} \tag{45}$$

With this definition, one can prove that the following elliptic equation on the graph $\mathcal{G}_h$ is well-posed [9, Section 2.3]:

$$\Delta_{\mathcal{G}_h} u_h = \frac{1}{2} f|_{\mathcal{G}_h} \tag{46}$$

In order to state the approximation results, we need to define the h_h^1 and ℓ_h^∞ norms on the grid $\mathcal{G}_h$:

$$\|u\|_{h_h^1}^2 \coloneqq \sum_{j \in J^h} \int_{e_j} \left[(u_j)^2 + (u_j')^2 \right] \mathrm{d}x;$$
$$\|u\|_{\ell_h^\infty} \coloneqq \operatorname{esssup}\{|u_h(x)| : x \in e_j \in E_h\}.$$

In these norms, one has an approximation result of order $\sqrt{h}$, which is the subject of the main theorem in this section:

Theorem 7 ([9, Corollary 3.6])**.** *Let $f \in W^{1,p}(\mathcal{S})$, with $p > 2$, such that f is zero at each corner of $\mathcal{S}$. Then the solution u of (44) has $H^3(\mathcal{S})$ regularity. Furthermore, there exists a constant $C > 0$ independent of h and f such that, if u_h is the solution of (46), the following error estimates hold:*

$$\|u_h - u|_{G_h}\|_{h_h^1} \leq C\sqrt{h}\|u\|_{H^3(\mathcal{S})}; \tag{47}$$
$$\|u_h - u|_{G_h}\|_{\ell^\infty} \leq C\sqrt{h}\|u\|_{H^3(\mathcal{S})}. \tag{48}$$

The meaning of the aforementioned result is that the Dirichlet problem on a square in $\mathbb{R}^2$ can be regarded as a limit of continuous equations on embedded networks, as the embedding progressively encompasses the domain. For similar findings on arbitrary domains, interested readers may refer to [9, Section 5]. Additionally, approximation results for the spectrum of operators on domains in $\mathbb{R}^2$ with the graph spectrum of embedded networks can be found in [55] and the references therein.

8 Interdependence of dynamical network models

In the last section we look closer at four major groups of networked models considered in the paper; namely those based purely on structure of combinatorial digraphs, or on dynamics: in vertices, on edges or on embedded edges. For all above concepts we trace both differences and similarities in their foundations, compare mathematical tools applied and assign them to the general mathematical field where they belong.

In order to apply the network paradigm one needs to observe a group of objects that interact one with another. The assignment of objects into mentioned groups may be related with their physical location, and then we talk about the graph which is embedded into $\mathbb{R}^n$ space. On the other hand, it may be based on any other common feature of the objects and then interaction does not have to possess physical representation. Specified interactions constitute a backbone of every networked model. In this study we indicate in many cases the difference in the role of interaction's

initiator and its recipient, hence the object that structures the model is a digraph.

Even though from mathematical perspective we are in the set theory, the combinatorial digraph provides the information about dynamics which is hidden in the structure, namely in the incidence matrices $\Phi^{\pm}$ and in weights of edges W. This characteristics can be described either in one moment in time, eg. when the process is at equilibrium point, or in several moments which allows for capturing the temporary state of a system.

In order to understand the process better one can define operators on digraphs. They can be of several natures, either purely related to the network structure (see (4) – (9)) or providing additional information ((21), (24), (25), (29), (30)); defined in vertices (eg. (7) – (9)) or on edges (eg. (21), (24), (25), (29), (30)) etc. The properties of operators such as boundedness, self-adjointness, positivity, irreducibility etc. provide additional information about the phenomenon such as connectivity of groups, symmetry or periodicity of interactions. Furthermore, one can define a functional, called a graph measure, acting from the network either to the subset of $\mathbb{R}$, in the case of global measures (eg. reciprocity or modularity), or to the subset of $\mathbb{R}^n/\mathbb{R}^m$, in the case of local measures (such as Finn cycling index or pagerank). All of these notions are examined in Section 4.

Having network operators defined, one can consider both linear and non-linear abstract Cauchy problems (ACP) generated by them, moving smoothly from algebraic methods to pure analysis. Depending on the type of an operator we arrive at ODE's defined in vertices (Section 5) or PDE's defined on edges (Section 6). Nevertheless, the classification is not that straightforward. If we allow for inhomogeneity of objects in vertices, we introduce an additional variable x extending the dimension of the vertex v_i, for example into dimension one in the simplest case. Then the functional space above the vertex can be defined and one can consider PDEs in vertices instead of ODE's. In this case an edge having a head in v_j and a tail in v_i may, for example, inform about mass' flow from one point at locally one dimensional metric space in the vertex v_i to another point in another vertex v_j, [2]. It can be obviously more complex taking for instance non-local transfers, [3]. This reasoning can be easily extended to vertices of arbitrary dimension.

In order to state the relation of dynamics in locally one dimensional vertices to corresponding dynamic defined on the edges of metric graph one needs to ensure that it is possible to build a metric graph based on network relations, proposed by incidence matrices $\Phi^{\pm}$. Figuratively speaking, if we, for instance, associate vertex v_i with interval $[0, l_i]$, then we need to glue ends of this interval with ends of other intervals related to the vertices that are adjacent to v_i. The endpoints of intervals constitute new vertices and intervals themselves become edges of a newly defined metric graph. If such a procedure holds, we say that the problem is graph realisable, [1]. However, it is always possible to represent PDE on metric graph edges by the PDEs in vertices framework.

Additionally, it is sometimes possible to relate PDEs on metric graph's edges with ODEs in vertices by methods of aggregation such as asymptotic state lumping [2]. This process can be interpreted also as the aggregation

of the process in the micro scale into the macro model.

There are even more relations between presented notions. Among all algebraic methods that serve to examine operators on networks, we emphasize spectral theory which has become a standard tool in dynamical properties analysis. From one hand, people compare the spectrum of network operators and define graph measures based on them (eg. eigenvector centrality). From another, finding the spectrum of a semigroup allows to obtain long-time behaviour of an evolution equation. Finally, examining the long-time behaviour of the process or its point evaluation in time is a well-known method of recovering the weights of initial combinatorial digraphs from observed phenomenon.

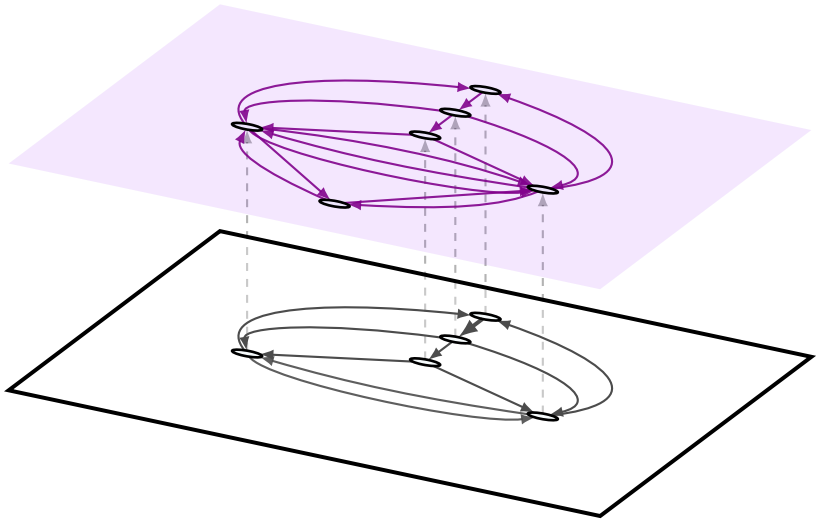

Figure 5: Two-layer digraph presenting interrelations between different network models considered in the paper. The upper layer is related to embedded digraphs while lower with unembbeded ones. Consequently, in upper layer there is one more vertex representing models defined on the whole metric space, in which models are embedded. Furthermore there are additional edges that have no counterparts in lower layer, that represent space discretisation/aggregation.

At the end of these considerations let us return to the concept of a network that is embedded into a larger vector space, which can sometimes be a natural way of description. It allows us to introduce geometry, see planar embedding of a digraph/metric graph in Subsection 3.2, instead of giving only the weighted relation between groups of objects. Furthermore, as presented in Subsection 7.1, in many cases the dynamics depends on the geometry and consequently PDEs on embedded edges and ODEs/PDEs in embedded vertices may constitute more complex dynamics compared to their unembedded counterparts.

The mutual relations stated for combinatorial graphs, PDEs on edges and ODEs/PDEs in vertices hold for the case of embedded networks. Furthermore, adding the geometry, one can consider their relation with

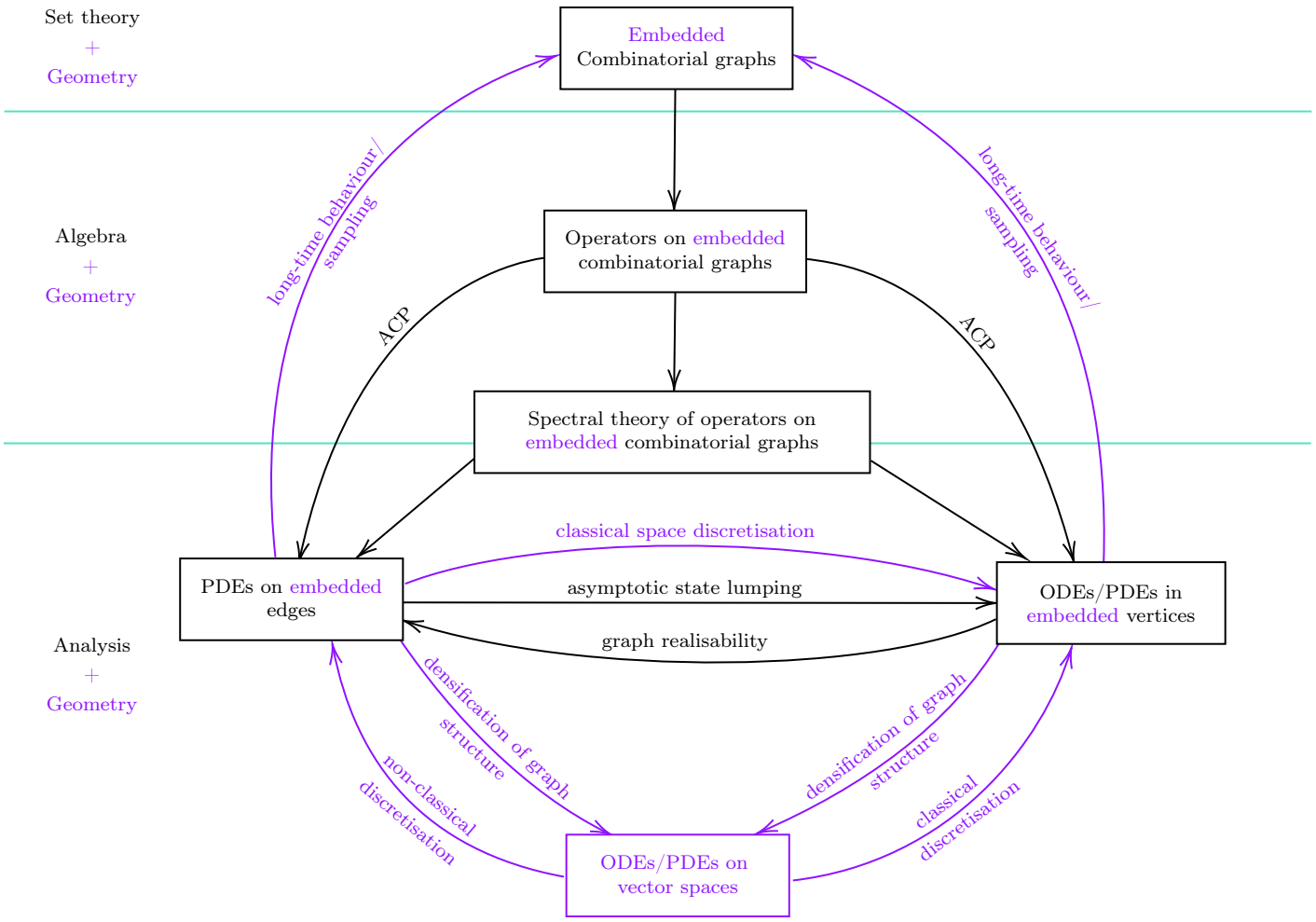

Figure 6: Diagram illustrating interrelation between different network models considered in the paper. Two-layered structure shown in Fig. 5 has been projected into the plane. To indicate original layer-structure, the elements (vertices, edges) that appear in both layers remained black while the elements unique to the upper layer are presented in violet.

the reference vector space. Namely, network models can be regarded as specific discretisation of the system of PDEs/ODEs defined on the whole vector space like in the Subsection 7.2. For instance, starting from a planar system one can choose standard discretization to obtain a set of vertices in which the system evolves, hence the model on vertices. On the other hand, using non-standard discretisation by describing evolution along locally one dimensional spaces we arrive at a metric graph model.

Finally, discretizing the latter by considering the dynamical process at vertices of a metric graph only, we return to the combinatorial graph system.

We present all mentioned relations in the diagram 5 having a form of two-layered digraph. In the lower (white) layer there are objects related to unembedded networks while on the upper (violet) one, their embedded counterparts are captured. There is one additional vertex in upper layer representing models defined on the whole vector space. Each vertex from the lower layer has a directed link with its embedded counterpart, and the link informs about the embedding into vector space. The relations shared by both groups of objects are presented by black arrows whereas relation specific for embedded networks (the upper layer) is by violet links. Figure 6 presents an aggregated model where both layers are included and violet edges are the ones specific to the upper layer. Finally, on the left hand side one can find the mathematical field where the object belongs. Assignment presented in violet again informs about additional field characteristics to the embedded objects.

References

[1] J. Banasiak and A. Falkiewicz. Some transport and diffusion processes on networks and their graph realizability. *Appl. Math. Lett.*, 45:25–30, 2015.

[2] J. Banasiak, A. Falkiewicz, and P. Namayanja. Asymptotic state lumping in transport and diffusion problems on networks with applications to population problems. *Math. Models Methods Appl. Sci.*, 26:215–247, 2016.

[3] J. Banasiak, A. Goswami, and S. Shindin. Aggregation in age and space structured opulation models: an asymptotic analysis approach. *J. Evol. Equ.*, 11:121–154, 2011.

[4] J. Banasiak and P. Namayanja. Asymptotic behaviour of flows on reducible networks. *Netw. Heterog. Media*, 9:197–216, 2014.

[5] J. Bang-Jensen and G. Gutin. *Digraphs.* Springer Monographs in Mathematics. Springer-Verlag London, Ltd., London, 2001. Theory, algorithms and applications.

[6] A. Barrat, M. Barthélemy, and A. Vespignani. *Dynamical processes on complex networks.* Cambridge University Press, 2008.

[7] A. Bátkai, M. Kramar Fijavž, and A. Rhandi. *Positive operator semigroups: From finite to infinite dimensions*, volume 257 of *Operator Theory: Advances and Applications.* Birkhäuser/Springer, Cham, 2017.

[8] F. Bayazit, B. Dorn, and M. Kramar Fijavž. Asymptotic periodicity of flows in time-depending networks. *Netw. Heterog. Media*, 8:843–855, 2013.

[9] M. Bourlard-Jospin, S. Nicaise, and J. Venel. Approximation of the two-dimensional Dirichlet problem by continuous and discrete problems on one-dimensional networks. *Confluentes Math.*, 7:13–33, 2015.

[10] Ch. Budde and M. Kramar Fijavž. Well-posedness of non-autonomous transport equation on metric graphs. *Semigroup Forum*, pages 1–16, 03 2024.

[11] M. Budišić, R. Mohr, and I. Mezić. Applied Koopmanism. *Chaos*, 22:047510–047510, 2012.

[12] M. Cartier van Dissel, P. Gora, and D. Manea. A Payne-Whitham model of urban traffic networks in the presence of traffic lights and its application to traffic optimisation. 2024.

[13] S. W. Chen, C. B. Yang, and Y. H. Peng. Algorithms for the traffic light setting problem on the graph model. In *Proceedings of the 12th Conference on Artificial Intelligence and Applications*. TAAI, 2007.

[14] F. R. Chung. *Spectral graph theory*, volume 92. American Mathematical Soc. Providence, RI, 1997.

[15] M. Cinelli, G. Ferraro, Iovanella A., and G. Rotundo. Assessing the impact of incomplete information on the resilience of financial networks. *Ann. Oper. Res.*, pages 1–25, 2019.

[16] A. M. D'Arcangelis, S. Levantesi, and G. Rotundo. A complex networks approach to pension funds. *J. Bus. Res*, pages 687–702, 2021.

[17] BIS database. https://www.bis.org/statistics/lbs_globalcoverage.pdf.

[18] D. P. Dewey. Measuring social interaction during study abroad: Quantitative methods and challenges. *System*, 71:49–59, 2017.

[19] G. E. Dullerud and F. Paganini. *A course in robust control theory: a convex approach*, volume 36. Springer Science & Business Media, 2013.

[20] K.-J. Engel and M. Kramar Fijavž. Waves and diffusion on metric graphs with general vertex conditions. *Evol. Equ. Control Theory*, 8:633–661, 2019.

[21] K.-J. Engel and M. Kramar Fijavž. Flows on metric graphs with general boundary conditions. *J. Math. Anal. Appl.*, 513:Paper No. 126214, 27, 2022.

[22] S. Epskamp, D. Borsboom, and E. I. Fried. Estimating psychological networks and their accuracy: A tutorial paper. *Behav. Res. Methods*, 50:195–212, 2018.

[23] M. Kramar Fijavž, D. Mugnolo, and S. Nicaise. Linear hyperbolic systems on networks: well-posedness and qualitative properties. *ESAIM Control Optim. Calc. Var.*, 27:Paper No. 7, 46 pp., 2021.

[24] M. Kramar Fijavž and A. Puchalska. Semigroups for dynamical processes on metric graphs. *Philos. Trans. Roy. Soc. A*, 378:20190619, 16, 2020.

[25] M. Kramar Fijavž, D. Mugnolo, and E. Sikolya. Variational and semigroup methods for waves and diffusion in networks. *Appl. Math. Optim.*, 55:219–240, 2007.

[26] J. T. Finn. Measures of ecosystem structure and function derived from analysis of flows. *J. Theor. Biol.*, 56:363–380, 1976.

[27] L. Freeborn, S. Andringa, G. Lunansky, and J. Rispens. Network analysis for modeling complex systems in sla research. *Stud. Second Lang. Acquis.*, 44:1–32, 2022.

[28] P. Ghisellini, C. Cialani, and S. Ulgiati. A review on circular economy: the expected transition to a balanced interplay of environmental and economic systems. *J. Clean. Prod.*, 114:11–32, 2016.

[29] M. Gulina and A. Mauroy. Spectral identification of networks with generalized diffusive coupling. In *Proceedings of the 25th International Symposium on Mathematical Theory of Networks and Systems*, 2022.

[30] B. Hannon. The structure of ecosystems. *J. Theor. Biol.*, 41:535–546, 1973.

[31] A. Hasegawa. *The social lives of study abroad: Understanding second language learners' experiences through social network analysis and conversation analysis*. Routledge, 2019.

[32] A. Hayek, S. Nicaise, Z. Salloum, and A. Wehbe. Existence, uniqueness and stabilization of solutions of a generalized telegraph equation on star shaped networks. *Acta Appl. Math.*, 170:823–851, 2020.

[33] M. Iskrzyński, F. Janssen, F. Picciolo, B. Fath, and F. Ruzzenenti. Cycling and reciprocity in weighted food webs and economic networks. *J. Ind. Ecol.*, 26:838–849, 2022.

[34] A. Jarynowski, M. B. Paradowski, and A. Buda. Modelling communities and populations: An introduction to computational social science. *Studia Metodologiczne – Dissertationes Methodologicae*, 39:123–152, 2019.

[35] S. E. Jørgensen, B. Fath, S. Nielsen, F. Pulselli, D. Fiscus, and S. Bastianoni. *Flourishing Within Limits to Growth Following nature's way*. 08 2015.

[36] K. Kennedy Terry. *Social networks*. Routledge, 2022.

[37] B. O. Koopman. Hamiltonian systems and transformation in Hilbert space. *Proceedings of the National Academy of Sciences of the United States of America*, 17:315, 1931.

[38] A. Kotsialos, M. Papageorgiou, C. Diakaki, Y. Pavlis, and F. Middelham. Traffic flow modeling of large-scale motorway networks using the macroscopic modeling tool metanet. *IEEE Trans. Intell. Transp. Syst.*, 3:282–292, 2002.

[39] M. Kovács and E. Sikolya. On the parabolic Cauchy problem for quantum graphs with vertex noise. *Electron. J. Probab.*, 28:Paper No. 74, 20, 2023.

[40] M. Kramar and E. Sikolya. Spectral properties and asymptotic periodicity of flows in networks. *Math. Z.*, 249:139–162, 2005.

[41] A. Layton, B. Bras, and M. Weissburg. Designing Industrial Networks Using Ecological Food Web Metrics. *Environ. Sci. Technol.*, 50:11243–11252, 2016.

[42] A. Layton, B. Bras, and M. Weissburg. Ecological principles and metrics for improving material cycling structures in manufacturing networks. *J. Manuf. Sci. Eng.*, 138:1–12, 2016.

[43] A. Layton, J. Reap, B. Bras, and M. Weissburg. Correlation between Thermodynamic Efficiency and Ecological Cyclicity for Thermodynamic Power Cycles. *PLoS ONE*, 7:1–7, 2012.

[44] W. Leontief. The economy as a circular flow. *Struct. Chang. Econ. Dyn.*, 2:181 – 212, 1991.

[45] F. L. Lewis, H. Zhang, K. Hengster-Movric, and A. Das. *Cooperative control of multi-agent systems: optimal and adaptive design approaches*. Springer Science & Business Media, 2013.

[46] A. Lonc, S. Nicaise, and A. Puchalska. Impulsive vs network transport - the first approach. 2024.

[47] T. Mátrai and E. Sikolya. Asymptotic behavior of flows in networks. *Forum Math.*, 19:429–461, 2007.

[48] A. Mauroy and J. M. Hendrickx. Spectral identification of networks using sparse measurements. *SIAM J. Appl. Math.*, 16:479–513, 2017.

[49] R. Mitchell, N. Tracy-Ventura, and K. McManus. *Social interaction, identity and language learning during residence abroad*. The European Second Language Association, 2015.

[50] R. F. Mitchell, N. Tracy–Ventura, and K. McManus. *Anglophone students abroad: Identity, social relationships and language learning*. Routledge, 2017.

[51] D. Mugnolo. *Semigroup methods for evolution equations on networks*. Understanding Complex Systems. Springer, Cham, 2014.

[52] I. Nakić, D. Tolić, Z. Tomljanović, and I. Palunko. Numerically efficient H_∞ analysis of cooperative multi-agent systems. *J. Frank. Inst.*, 359:9110–9128, 2022.

[53] S. Nicaise. Some results on spectral theory over networks, applied to nerve impulse transmission. In *Orthogonal polynomials and applications (Bar-le-Duc, 1984)*, volume 1171 of *Lecture Notes in Math.*, pages 532–541. Springer, Berlin, 1985.

[54] S. Nicaise. Control and stabilization of 2×2 hyperbolic systems on graphs. *Math. Control Relat. Fields*, 7:53–72, 2017.

[55] S. Nicaise and O. Penkin. Relationship between the lower frequency spectrum of plates and networks of beams. *Math. Methods Appl. Sci.*, 23:1389–1399, 2000.

[56] M. B. Paradowski, P. Bródka, and M. Czuba. Peer interaction dynamics and l2 learning trajectories during study abroad: A longitudinal investigation using dynamic computational social network analysis. *Language Learning*, 2024, in press.

[57] M. B. Paradowski, Cierpich-Kozieł, C.-C. A., Chen, and J. K. Ochab. How output outweighs input and interlocutors matter for study-abroad sla: Computational social network analysis of learner interactions. *Mod. Lang. J.*, 106:694–725, 2022.

[58] M. B. Paradowski, A. Jarynowski, K. Czopek, and M. Jelińska. Peer interactions and second language learning: The contributions of social network analysis in study abroad vs at-home environments. In R. Mitchell and H. Tyne, editors, *Language, Mobility and Study Abroad in the Contemporary European Context*, page 99–116. Routledge, 2021.

[59] M. B. Paradowski, A. Jarynowski, M. Jelińska, and K. Czopek. Out-of-class peer interactions matter for second language acquisition during short-term overseas sojourns: The contributions of social network analysis [selected poster presentations from the american association of applied linguistics conference, denver, usa, march 2020]. *Lang. Teach.*, 54:139–143, 2021.

[60] M. B. Paradowski and M. Jelińska. The predictors of l2 grit and their complex interactions in online foreign language learning: Motivation, self-directed learning, autonomy, curiosity, and language mindsets. *Comput. Assist. Lang. Learn.*, 2023.

[61] M. B. Paradowski and Ł. Jonak. Diffusion of linguistic innovation as social coordination. *Psychol. Lang. Commun.*, 16:53–64, 2012.

[62] Ł. Pawluczuk and M. Iskrzyński. Food web visualisation: Heat map, interactive graph and animated flow network. *Methods Ecol. Evol.*, 14:57–64, 2023.

[63] H. J. Payne. Models of freeway traffic and control. In *Mathematical Models of Public Systems, Simulation Council Proceedings*, pages 51 – 61, 1971.

[64] E. J. Schwarz and K. W. Steininger. Implementing nature's lesson: the industrial recycling network enhancing regional development. *J. Clean. Prod.*, 5(1-2):47–56, 1997.

[65] J. H. Tu, C. W. Rowley, D. M. Luchtenburg, S. L. Brunton, and J. N. Kutz. On dynamic mode decomposition: Theory and applications. *J. Comput. Dyn.*, 1:391 – 421, 2014.

[66] J. von Below. A characteristic equation associated to an eigenvalue problem on c^2-networks. *Linear Algebra and Appl.*, 71:309–325, 1985.

[67] K. Webster. *The circular economy: A wealth of flows.* Ellen MacArthur Foundation Publishing, 2017.

[68] G. B. Whitham. *Linear and nonlinear waves.* Pure and Applied Mathematics (New York). John Wiley & Sons, Inc., New York, 1999. Reprint of the 1974 original, A Wiley-Interscience Publication.